

Thermal Activation of Hydrocarbon C–H Bonds by Tungsten Alkylidene Complexes

Craig S. Adams, Peter Legzdins,* and Elizabeth Tran

Contribution from the Department of Chemistry, The University of British Columbia, Vancouver, British Columbia, Canada V6T 1Z1

Received July 6, 2000

Abstract: Thermal activation of $\text{Cp}^*\text{W}(\text{NO})(\text{CH}_2\text{CMe}_3)_2$ (**1**) in neat hydrocarbon solutions transiently generates the neopentylidene complex, $\text{Cp}^*\text{W}(\text{NO})(=\text{CHCMe}_3)$ (**A**), which subsequently activates solvent C–H bonds. For example, the thermolysis of **1** in tetramethylsilane and perdeuteriotetramethylsilane results in the clean formation of $\text{Cp}^*\text{W}(\text{NO})(\text{CH}_2\text{CMe}_3)(\text{CH}_2\text{SiMe}_3)$ (**2**) and $\text{Cp}^*\text{W}(\text{NO})(\text{CHDCMe}_3)[\text{CD}_2\text{Si}(\text{CD}_3)_3]$ (**2-*d*₁₂**), respectively, in virtually quantitative yields. The neopentylidene intermediate **A** can be trapped by PMe_3 to obtain $\text{Cp}^*\text{W}(\text{NO})(=\text{CHCMe}_3)(\text{PMe}_3)$ in two isomeric forms (**4a–b**), and in benzene, **1** cleanly forms the phenyl complex $\text{Cp}^*\text{W}(\text{NO})(\text{CH}_2\text{CMe}_3)(\text{C}_6\text{H}_5)$ (**5**). Kinetic and mechanistic studies indicate that the C–H activation chemistry derived from **1** proceeds through two distinct steps, namely, (1) rate-determining intramolecular α -H elimination of neopentane from **1** to form **A** and (2) 1,2-cis addition of a substrate C–H bond across the $\text{W}=\text{C}$ linkage in **A**. The thermolysis of **1** in cyclohexane in the presence of PMe_3 yields **4a–b** as well as the olefin complex $\text{Cp}^*\text{W}(\text{NO})(\eta^2\text{-cyclohexene})(\text{PMe}_3)$ (**6**). In contrast, methylcyclohexane and ethylcyclohexane afford principally the allyl hydride complexes $\text{Cp}^*\text{W}(\text{NO})(\eta^3\text{-C}_7\text{H}_{11})(\text{H})$ (**7a–b**) and $\text{Cp}^*\text{W}(\text{NO})(\eta^3\text{-C}_8\text{H}_{13})(\text{H})$ (**8a–b**), respectively, under identical experimental conditions. The thermolysis of **1** in toluene affords a surprisingly complex mixture of six products. The two major products are the neopentyl aryl complexes, $\text{Cp}^*\text{W}(\text{NO})(\text{CH}_2\text{CMe}_3)(\text{C}_6\text{H}_4\text{-3-Me})$ (**9a**) and $\text{Cp}^*\text{W}(\text{NO})(\text{CH}_2\text{CMe}_3)(\text{C}_6\text{H}_4\text{-4-Me})$ (**9b**), in approximately 47 and 33% yields. Of the other four products, one is the aryl isomer of **9a–b**, namely, $\text{Cp}^*\text{W}(\text{NO})(\text{CH}_2\text{CMe}_3)(\text{C}_6\text{H}_4\text{-2-Me})$ (**9c**) (~1%). The remaining three products all arise from the incorporation of *two* molecules of toluene; namely, $\text{Cp}^*\text{W}(\text{NO})(\text{CH}_2\text{C}_6\text{H}_5)(\text{C}_6\text{H}_4\text{-3-Me})$ (**11a**; ~12%), $\text{Cp}^*\text{W}(\text{NO})(\text{CH}_2\text{C}_6\text{H}_5)(\text{C}_6\text{H}_4\text{-4-Me})$ (**11b**; ~6%), and $\text{Cp}^*\text{W}(\text{NO})(\text{CH}_2\text{C}_6\text{H}_5)_2$ (**10**; ~1%). It has been demonstrated that the formation of complexes **10** and **11a–b** involves the transient formation of $\text{Cp}^*\text{W}(\text{NO})(\text{CH}_2\text{CMe}_3)(\text{CH}_2\text{C}_6\text{H}_5)$ (**12**), the product of toluene activation at the methyl position, which reductively eliminates neopentane to generate the C–H activating benzylidene complex $\text{Cp}^*\text{W}(\text{NO})(=\text{CHC}_6\text{H}_5)$ (**B**). Consistently, the thermolysis of independently prepared **12** in benzene and benzene-*d*₆ affords $\text{Cp}^*\text{W}(\text{NO})(\text{CH}_2\text{C}_6\text{H}_5)(\text{C}_6\text{H}_5)$ (**13**) and $\text{Cp}^*\text{W}(\text{NO})(\text{CHDC}_6\text{H}_5)(\text{C}_6\text{D}_5)$ (**13-*d*₆**), respectively, in addition to free neopentane. Intermediate **B** can also be trapped by PMe_3 to obtain the adducts $\text{Cp}^*\text{W}(\text{NO})(=\text{CHC}_6\text{H}_5)(\text{PMe}_3)$ (**14a–b**) in two rotameric forms. From their reactions with toluene, it can be deduced that both alkylidene intermediates **A** and **B** exhibit a preference for activating the stronger aryl sp^2 C–H bonds. The C–H activating ability of **B** also encompasses aliphatic substrates as well as it reacts with tetramethylsilane and cyclohexanes in a manner similar to that summarized above for **A**. All new complexes have been characterized by conventional spectroscopic methods, and the solid-state molecular structures of **4a**, **6**, **7a**, **8a**, and **14a** have been established by X-ray diffraction methods.

Introduction

The development of efficient, selective, and catalytic methods for the direct conversion of hydrocarbon feedstocks into functionalized organic compounds is an important ongoing challenge in modern chemistry.¹ Considerable progress in this regard has been made in the field of organometallic chemistry where numerous metal-containing complexes have been found to effect selective intermolecular C–H bond activations.^{1,2} Notable examples include late-transition-metal complexes that

oxidatively add C–H bonds to the metal center,³ transition-metal, lanthanide, and actinide complexes that facilitate C–H activation via M–C σ -bond metathesis,⁴ and early- to mid-transition-metal complexes that add C–H bonds across a M=NR linkage.⁵ A fundamental understanding of the discrete C–H activation processes has been acquired for many of these

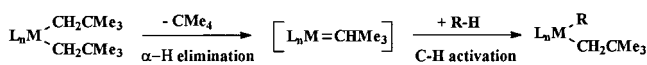
(1) (a) *Activation and Functionalization of Alkanes*; Hill, C. L., Ed.; Wiley-Interscience: New York, 1989. (b) Crabtree, R. H. *Chem. Rev.* **1995**, *95*, 987–1007.

(2) For leading reviews, see: (a) Shilov, A. E.; Shul'pin, G. B. *Chem. Rev.* **1997**, *97*, 2879–2932. (b) Arndtsen, B. A.; Bergman, R. G.; Mobley, T. A.; Peterson, T. H. *Acc. Chem. Res.* **1995**, *28*, 154–162. (c) Stahl, S. S.; Labinger, J. A.; Bercaw, J. E. *Angew. Chem., Intl. Ed. Engl.* **1998**, *37*, 2180–2192. (d) Crabtree, R. H. *Chem. Rev.* **1985**, *85*, 245–269.

(3) (a) Janowicz, A. H.; Bergman, R. G. *J. Am. Chem. Soc.* **1983**, *105*, 3929–3939. (b) Hoyano, J. K.; Graham, W. A. G. *J. Am. Chem. Soc.* **1982**, *104*, 3723–3725. (c) Jones, W. D.; Feher, F. J. *Acc. Chem. Res.* **1989**, *22*, 91–100. (d) Arndtsen, B. A.; Bergman, R. G. *Science* **1995**, *270*, 1970–1973. (e) Wick, D. D.; Goldberg, K. I. *J. Am. Chem. Soc.* **1997**, *119*, 10235–10236 and references therein.

(4) (a) Erker, G. *J. Organomet. Chem.* **1977**, *134*, 189–202. (b) Watson, P. L.; Marshall, G. W. *Acc. Chem. Res.* **1985**, *18*, 51–56. (c) Fendrick, C. M.; Marks, T. J. *J. Am. Chem. Soc.* **1986**, *108*, 425–437. (d) Thompson, M. E.; Baxter, S. M.; Bulls, R.; Burger, B. J.; Nolan, M. C.; Santarsiero, B. D.; Schaefer, W. P.; Bercaw, J. E. *J. Am. Chem. Soc.* **1987**, *109*, 203–219. (e) Debad, J. D.; Legzdins, P.; Lumb, S. A.; Rettig, S. J.; Batchelor, R. J.; Einstein, F. W. B. *Organometallics* **1999**, *18*, 3414–3428.

Scheme 1



complexes, and the chemistry of select systems has been significantly advanced toward efficient, catalytic functionalizations.⁶

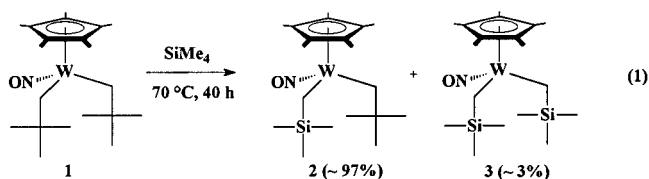
In recent years, organometallic C–H activation research has expanded to include a small class of complexes that intermolecularly activate C–H bonds via their addition across the M=C bond of an alkylidene intermediate.⁷ In each case, the reactive species is a transient neopentylidene complex generated thermally in situ from a *cis*-bis(neopentyl) precursor by the microscopic reverse of the C–H activation reaction, namely, α -H elimination of neopentane (Scheme 1). The neopentylidene intermediates generated from (2,6-*i*-Pr₂C₆H₃N)₂Cr(CH₂CMe₃)₂⁸ and Cp^{*}Ti(CH₂CMe₃)₂ [Cp^{*} = C₅H₅ (Cp) or C₅Me₅ (Cp^{*})]⁹ in this manner activate an aryl sp² C–H bond of benzene to afford the corresponding phenyl neopentyl complexes. There is also strong evidence for the activation of alkane and arene C–H bonds by a neopentylidene intermediate during the thermal decomposition of Ti(CH₂CMe₃)₄.¹⁰ Finally, we have observed that the thermolysis of Cp^{*}W(NO)(CH₂CMe₃)₂ (**1**) leads to the formation of a neopentylidene complex, namely, Cp^{*}W(NO)-(=CHCMe₃) (**A**), which activates the primary and secondary C–H bonds of tetramethylsilane and cyclohexane, respectively.¹¹ To date it appears that neopentylidene complex **A** is unique in its ability to activate aliphatic C–H bonds to yield isolable, well-defined products.

With the intention of advancing the understanding of alkylidene-mediated C–H activation processes, we now report the results of our survey of the thermal chemistry of **1** in various solvents. Included in this report are details concerning the previously communicated activation of tetramethylsilane and cyclohexane, as well as additional mechanistic information concerning the formation and reactivity of intermediate **A**. We have also extended the scope of this chemistry to encompass select alkane and arene substrates in an attempt to assess the relative intramolecular selectivities of **A** for aliphatic and aromatic C–H bonds. During these studies, we have discovered that additional C–H activation chemistry can occur depending

on the nature of the solvent employed. Observed modes of reactivity include the spontaneous functionalization of the activated substrates by dehydrogenation and the formation of a new benzylidene complex that is also capable of selectively activating both alkane and arene C–H bonds. To the best of our knowledge, this constitutes the first detailed study of the activation of C–H bonds by alkylidene complexes.

Results and Discussion

A. Generation of Cp^{*}W(NO)=(=CHCMe₃) (A**) and the Mechanism by Which It Activates C–H Bonds. Activation of Tetramethylsilane.** The thermolysis of **1** for 40 h at 70 °C in neat tetramethylsilane results in the clean formation (~97% as judged by ¹H NMR spectroscopy) of the known¹² mixed alkyl complex, Cp^{*}W(NO)(CH₂CMe₃)(CH₂SiMe₃) (**2**) (eq 1). Com-



plex **2** is clearly derived from **1** via the activation of an sp³ aliphatic C–H bond of a solvent molecule. Several plausible mechanisms could account for this transformation. These include direct σ -bond metathesis or homolytic cleavage mechanisms, as well as pathways involving metallacyclic or alkylidene intermediates via intramolecular α -H, γ -H, or Cp^{*}-H abstractions. Our mechanistic studies are only consistent with the formation of the alkylidene intermediate.

Monitoring by ¹H NMR spectroscopy indicates that the thermolysis of **1** in perdeuteriotetramethylsilane at 70 °C for 40 h produces free neopentane (1 equiv) and Cp^{*}W(NO)-(CHDCMe₃)[CD₂Si(CD₃)₃] (**2-d**₁₂). Complex **2-d**₁₂ can be isolated in high yield (93%) by crystallization from pentane. It exhibits a singlet in its ¹H NMR spectrum for the anticlinal methylene hydrogen atom (with respect to the new M–C bond)¹³ and a 1:1:1 triplet in its ¹³C{¹H} NMR spectrum for the methylene carbon of the neopentyl ligand. In addition, there is a broad singlet in its ²H{¹H} NMR spectrum that corresponds to the deuteron at the synclinal neopentyl methylene position. There are no other resonances in the ²H{¹H} NMR spectrum in the regions for the Cp^{*} ligand or the *tert*-butyl or anticlinal methylene positions of the neopentyl ligand. This exclusive and stereospecific deuterium incorporation is consistent with the 1,2-*cis* addition of C–D across the M=CHR linkage of a neopentylidene intermediate. The stereospecificity also indicates that C–H(D) activation occurs from only one of the two possible alkylidene isomers,¹⁴ namely, the isomer with anticlinal Cp^{*} and ^tBu groups.¹⁵ The C–H(D) activation step appears to be irreversible since isolated **2-d**₁₂ does not convert to **2** after heating in protiotetramethylsilane (70 °C, 40 h). However, **2** and **2-d**₁₂ do react further with tetramethylsilane under the

(12) Debad, J. D.; Legzdins, P.; Batchelor, R. J.; Einstein, F. W. B. *Organometallics* **1993**, *12*, 2094–2102.

(13) The relative stereochemistry of the methylene protons for the alkyl ligands has been ascertained by ¹H–¹H NOE difference spectroscopy (see Experimental Section).

(14) Recent theoretical calculations have shown that the ground-state conformation of the model compound CpW(NO)=CH₂ has a pyramidal geometry similar to CpW(NO)(PMe₃)=CH₂, with *syn* and anticlinal orientations of the methylene H's: Smith, K. M.; Poli, R.; Legzdins, P. *Chem. Eur. J.* **1999**, *5*, 1598–1608.

(15) If C–H activation was also occurring concomitantly from the other isomer with synclinal ^tBu/Cp^{*} geometry, then deuterium incorporation would be observed at the anticlinal methylene position.

(5) (a) Schaller, C. P.; Wolczanski, P. T. *Inorg. Chem.* **1993**, *32*, 131–144. (b) Schaller, C. P.; Cummins, C. C.; Wolczanski, P. T. *J. Am. Chem. Soc.* **1996**, *118*, 591–611. (c) Bennett, J. L.; Wolczanski, P. T. *J. Am. Chem. Soc.* **1997**, *119*, 10696–10719. (d) Schaefer, D. F., II; Wolczanski, P. T. *J. Am. Chem. Soc.* **1998**, *120*, 4881–4882. (e) With, J.; Horton, A. D. *Angew. Chem., Intl. Ed. Engl.* **1993**, *32*, 903–905. (f) Walsh, P. J.; Hollander, F. J.; Bergman, R. G. *Organometallics* **1993**, *12*, 3705–3723. (g) Lee, S. Y.; Bergman, R. G. *J. Am. Chem. Soc.* **1995**, *117*, 5877–5878.

(6) For example, see: (a) Chen, H.; Schlecht, S.; Semple, T. C.; Hartwig, J. F. *Science* **2000**, *287*, 1995–1997. (b) Liu, F.; Pak, E. B.; Singh, B.; Jensen, C. M.; Goldman, A. S. *J. Am. Chem. Soc.* **1999**, *121*, 4086–4087. (c) Periana, R. A.; Taube, D. J.; Gamble, S.; Taube, H.; Satoh, T.; Fujii, H. *Science* **1998**, *280*, 560–564.

(7) There are several examples of *intramolecular* C–H activation by alkylidene complexes: (a) Vilardo, J. S.; Lockwood, M. A.; Hanson, L. G.; Clark, J. R.; Parkin, B. C.; Fanwick, P. E.; Rothwell, I. P. *J. Chem. Soc., Dalton Trans.* **1997**, 3353–3362 and references therein. (b) McDade, C.; Green, J. C.; Bercaw, J. E. *Organometallics* **1982**, *1*, 1629–1634. (c) Bulls, A. R.; Schaefer, W. P.; Serfas, M.; Bercaw, J. E. *Organometallics* **1987**, *6*, 1219–1226. (d) van Doorn, J. A.; van der Heijden, H.; Orpen, A. G. *Organometallics* **1994**, *13*, 4271–4277. (e) Duncalf, D. J.; Harrison, R. J.; McCamley, A.; Royan, B. W. *J. Chem. Soc., Chem. Commun.* **1995**, 2421–2422.

(8) Coles, M. P.; Gibson, V. C.; Clegg, W.; Elsegood, M. R. J.; Porrelli, P. A. *J. Chem. Soc., Chem. Commun.* **1996**, 1963–1964.

(9) van der Heijden, H.; Hessen, B. J. *Chem. Soc., Chem. Commun.* **1995**, 145–146.

(10) Cheon, J.; Rogers, D. M.; Girolami, G. S. *J. Am. Chem. Soc.* **1997**, *119*, 6804–6813.

(11) Tran, E.; Legzdins, P. *J. Am. Chem. Soc.* **1997**, *119*, 5071–5072.

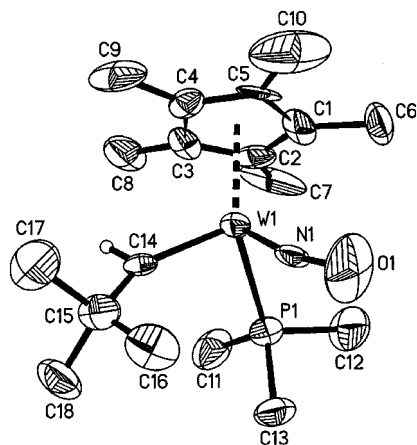
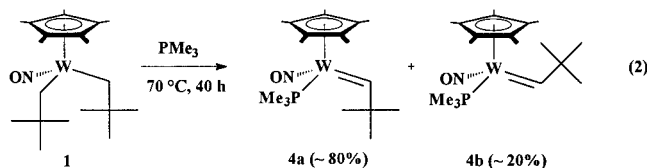


Figure 1. ORTEP plot of the solid-state molecular structure of $\text{Cp}^*\text{W}(\text{NO})=\text{CHCMe}_3(\text{PMe}_3)$ (**4a**) with 50% probability ellipsoids. Selected bond lengths (Å) and angles (deg): $\text{W}(1)-\text{C}(14) = 1.961(9)$, $\text{N}(1)-\text{O}(1) = 1.22(2)$, $\text{W}(1)-\text{N}(1)-\text{O}(1) = 163.3(14)$, $\text{W}(1)-\text{C}(14)-\text{C}(15) = 144.7(11)$, and $\text{N}(1)-\text{W}(1)-\text{C}(14)-\text{C}(15) = -7(3)$.

thermolysis conditions, albeit very slowly. For example, a trace amount ($\sim 3\%$) of a second product, $\text{Cp}^*\text{W}(\text{NO})(\text{CH}_2\text{SiMe}_3)_2$ (**3**), is detectable in the mixture obtained from the thermolysis of **1** in protiotetramethylsilane after 40 h (eq 1). The relative amount of **3** gradually increases upon prolonged heating of this mixture (to $\sim 8\%$ after an additional 40 h), thereby indicating that complex **3** is derived from **2** via the activation of a second solvent molecule. The implications of these results are discussed in due course (vide infra).

Trapping of the Neopentylidene Intermediate. The intermediacy of the neopentylidene complex **A** during the transformation of **1** to **2** is substantiated by its isolation in base-stabilized form from the thermolysis of **1** in neat trimethylphosphine. Two isomers of composition $\text{Cp}^*\text{W}(\text{NO})(=\text{CHCMe}_3)(\text{PMe}_3)$ (**4a**–**b**) occur in the final reaction mixture in $\sim 4:1$ ratio (eq 2).



The major isomer **4a** can be isolated in high yield (75%) as yellow plates from ether, and its solid-state molecular structure has been established by a single-crystal X-ray crystallographic analysis. The resulting ORTEP plot is shown in Figure 1. Notable metrical features of **4a** are its short $\text{W}(1)-\text{C}(14)$ bond distance of $1.961(9)$ Å and the obtuse $\text{W}-\text{C}(14)-\text{C}(15)$ bond angle of $144.7(11)^\circ$, both of which are consistent with the geometric parameters of neopentylidene ligands in other tungsten complexes.^{16,17} The neopentylidene ligand is oriented anticlinal to the Cp^* group, and the $\text{N}(1)-\text{W}(1)-\text{C}(14)-\text{C}(15)$ torsion angle is $-7(3)^\circ$. This configuration minimizes steric interactions in the metal's coordination sphere and maximizes the synergic π -bonding between the π -donor alkylidene and π -acceptor NO

(16) (a) Nugent, W. A.; Mayer, J. M. *Metal-Ligand Multiple Bonds*; Wiley: New York, 1988; Chapter 3. (b) Labinger, J. A.; Winter, M. J. In *Comprehensive Organometallic Chemistry II*; Abel, E. W., Stone, F. G. A., Wilkinson, G., Eds.; Elsevier Science Ltd: New York, 1995; Vol. 5, Chapter 5, pp 311–315.

(17) For the characterizations of the isostructural $\text{CpMo}(\text{NO})(\text{PMe}_3)(=\text{CHCMe}_3)$ alkylidene complexes, see: Legzdins, P.; Rettig, S. J.; Veltheer, J. E. *Organometallics* **1993**, *12*, 3575–3585.

Table 1. Rate Constants for the Thermolysis of **1** and **1-d₄**

compd	solvent	temp (°C)	av k_{obs} (s^{-1}) ^a
1	cyclohexane/ PMe_3	71	$5.3(1) \times 10^{-5}$
1	cyclohexane/ PMe_3	81	$1.6(1) \times 10^{-4}$
1	cyclohexane/ PMe_3	91	$4.7(1) \times 10^{-4}$
1	cyclohexane/ PMe_3	98	$1.1(1) \times 10^{-3}$
1-d ₄	cyclohexane/ PMe_3	91	$2.0(1) \times 10^{-4}$
1	benzene-d ₆	72	$4.6(1) \times 10^{-5}$

^a Errors reported to 3σ .

ligands.^{14,18} In solution, **4a** exhibits typical alkylidene NMR resonances at δ 11.25 ($^3J_{\text{HP}} = 3.6$ Hz) and 282.8 ($^1J_{\text{CH}} = 111$ Hz, $^2J_{\text{CP}} = 8.9$ Hz) for the α -proton and the α -carbon of the neopentylidene ligand, respectively.¹⁹ It also retains the anticlinal orientation of the ^tBu and Cp^* groups as indicated by NOE enhancements between the alkylidene α -H atom and the methyl H atoms of the Cp^* ring.

The second alkylidene product **4b** can be identified by spectroscopic analysis of the final reaction mixture. It is the geometric isomer of **4a** with a synclinal orientation of the ^tBu and Cp^* groups, as indicated by the diagnostic resonances at δ 12.87 ($^3J_{\text{HP}} = 4.4$ Hz) and δ 282.9 ($^2J_{\text{CP}} = 9.5$ Hz) in the ¹H and ¹³C NMR spectra and NOE enhancements between the ^tBu and Cp^* moieties. The isomers **4a**–**b** do not interconvert at room temperature on the NMR time scale, but do interconvert upon prolonged heating at elevated temperatures (vide infra) presumably by rotation around the $\text{M}=\text{C}$ bond.^{14,20}

Kinetic Studies of the Formation of 4a–b. The conversion of **1** to **4a**–**b** can be conveniently monitored by UV–visible spectroscopy in cyclohexane solutions containing an excess of PMe_3 (300 equiv). The reaction exhibits first-order kinetics for the loss of **1** over the temperature range of 71–98 °C (Table 1). An Eyring plot of the data affords the activation parameters $\Delta H^\ddagger = 114(7)$ kJ mol⁻¹ and $\Delta S^\ddagger = 3(12)$ J mol⁻¹ K⁻¹ (reported errors are 3σ). Both parameters lie within the range reported for other complexes that undergo rate-determining intramolecular α -H eliminations of alkane.^{7b,c} A primary deuterium kinetic isotope effect of 2.4(2) is observed when the PMe_3 -trapping reaction is conducted with $\text{Cp}^*\text{W}(\text{NO})(\text{CD}_2\text{CMe}_3)_2$ (**1-d₄**) at 91 °C, thereby confirming that the rate-determining step involves intramolecular cleavage of a methylene C–H(D) bond.²¹

Thermolysis of 1 in Benzene and Benzene-d₆. Additional mechanistic information can be gleaned from the thermolysis of **1** in benzene and benzene-d₆. In benzene, **1** cleanly forms the known phenyl complex $\text{Cp}^*\text{W}(\text{NO})(\text{CH}_2\text{CMe}_3)(\text{C}_6\text{H}_5)$ (**5**)¹² ($\sim 95\%$ as judged by ¹H NMR spectroscopy) by activation of an aryl sp² C–H bond.²² The thermolysis of **1** in benzene-d₆ affords free neopentane and $\text{Cp}^*\text{W}(\text{NO})(\text{CHDCMe}_3)(\text{C}_6\text{D}_5)$ (**5-**

(18) (a) Schilling, B. E. R.; Hoffman, R.; Faller, J. W. *J. Am. Chem. Soc.* **1979**, *101*, 592–598. (b) Gibson, V. C. *J. Chem. Soc., Dalton Trans.* **1994**, 1607–1618.

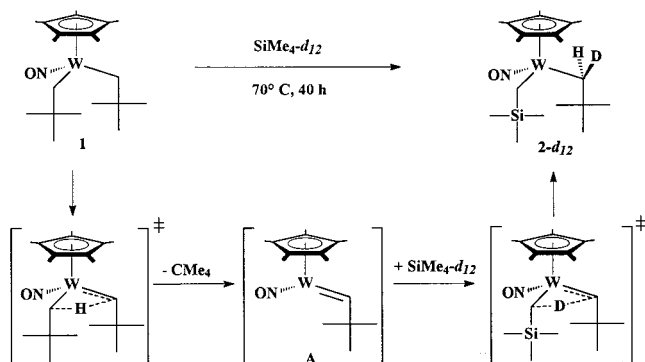
(19) Reference 16a; Chapter 4.

(20) Schofield, M. H.; Schrock, R. R.; Park, L. Y. *Organometallics* **1991**, *10*, 1844–1851.

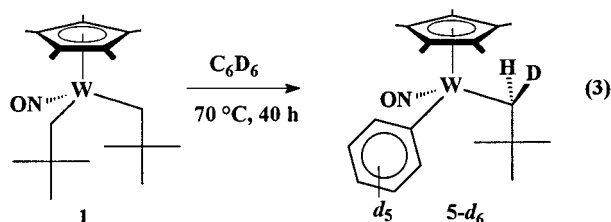
(21) The deuterium isotope effect for several other rate-determining α -H alkane elimination reactions lies in the range of 2–3: (a) Schrock, R. R.; Fellmann, J. D. *J. Am. Chem. Soc.* **1978**, *100*, 3359–3370 (b) Malatesta, V.; Ingold, K. U.; Schrock, R. R. *J. Organomet. Chem.* **1978**, *152*, C53–C56. (c) Fryzuk, M. D.; Duval, P. B.; Mao, S. S. S. H.; Zaworotko, M. J.; MacGillivray, L. R. *J. Am. Chem. Soc.* **1999**, *121*, 2478–2487. Also see refs 7b,c.

(22) Like complex **2**, complex **5** does react further with the solvent, although the reaction does not proceed at a significant rate under the thermolytic conditions employed for the conversion of **1** to **5**. Previous studies have shown that the thermolysis of pure **5** in benzene at 110 °C generates $\text{Cp}^*\text{W}(\text{NO})(\text{C}_6\text{H}_5)_2$, which decomposes thermally but can be trapped and isolated as the PMe_3 adduct in reasonable yield: Debad, J. D. Ph.D. Dissertation, University of British Columbia, 1989.

Scheme 2



d_6) with exclusive stereospecific deuterium incorporation at the synclinal methylene position of the neopentyl ligand (eq 3). The

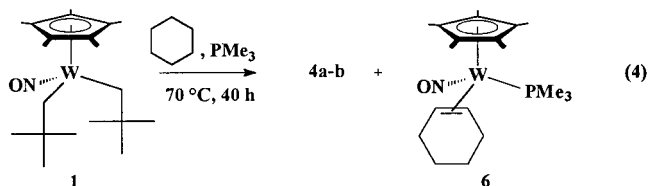


first-order rate constant obtained by ^1H NMR spectroscopy at 72.0°C is of the same magnitude as that obtained in cyclohexane/ PMe_3 solutions under comparable conditions (Table 1). This observation indicates that the presence of phosphine and the nature of the solvent do not significantly affect the rate of reaction, as expected for a process having an intramolecular rate-determining step.

Taken together, the labeling, trapping, and kinetic results verify that the C–H activation chemistry derived from **1** proceeds through two distinct steps: (1) formation of the neopentylidene complex **A** via rate-determining intramolecular α -H elimination of neopentane and (2) a 1,2-cis addition of R–H across the $\text{M}=\text{CHR}$ linkage of **A**. A simple two-step α -H abstraction mechanism is thus proposed, as illustrated in Scheme 2 for the conversion of **1** to **2-}d_{12}. However, other more complex mechanisms for the formation of **A**, such as synclinal α -H elimination to a discrete metal hydride/alkyl/alkylidene intermediate followed by neopentane reductive elimination,^{7b} cannot be ruled out at this time.**

B. Activation of Cyclohexanes by Neopentylidene Complex

A. Activation and Functionalization of Cyclohexane. The thermolysis of **1** in cyclohexane in the presence of a large excess of PMe_3 (i.e., >50 equiv) yields the alkylidene complexes **4a–b** as expected. However, as the relative amount of PMe_3 is decreased, the presence of a third product, namely, $\text{Cp}^*\text{W}(\text{NO})(\eta^2\text{-cyclohexene})(\text{PMe}_3)$ (**6**), can be detected in the ^1H NMR spectrum of the crude reaction mixture (eq 4). Complex **6** is



formed preferentially under “dilute” conditions (i.e., ≤ 12 equiv of PMe_3 for 1.0 mL of a 0.020 M solution of **1**) and can be separated from **4a–b** by chromatography on neutral alumina

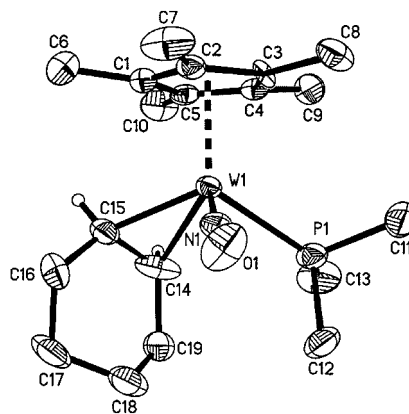


Figure 2. ORTEP plot of the solid-state molecular structure of $\text{Cp}^*\text{W}(\text{NO})(\eta^2\text{-cyclohexene})(\text{PMe}_3)$ (**6**) with 50% probability ellipsoids. Selected bond lengths (Å) and angles (deg): $\text{W}(1)\text{-C}(14) = 2.246(9)$, $\text{W}(1)\text{-C}(15) = 2.193(9)$, $\text{C}(14)\text{-C}(15) = 1.447(12)$, $\text{N}(1)\text{-W}(1)\text{-C}(14) = 105.8(3)$, $\text{N}(1)\text{-W}(1)\text{-C}(15) = 96.3(3)$, $\text{W}(1)\text{-N}(1)\text{-O}(1) = 172.6(6)$, and $\text{N}(1)\text{-W}(1)\text{-C}(14)\text{-C}(15) = 79.8(5)$.

and isolated as pale yellow needles in moderate yield (38%) by crystallization from ether/hexanes.

A single-crystal X-ray crystallographic analysis of **6** reveals a solid-state molecular structure (Figure 2) that is similar to those of the isoelectronic $[\text{CpRe}(\text{NO})(\text{alkene})\text{PPh}_3]^+$ cationic complexes previously studied by Gladysz et al.²³ The η^2 -cyclohexene ligand possesses some metallacyclopropane character, as indicated by the $\text{C}(14)\text{-C}(15)$ bond length of $1.447(12)$ Å that is intermediate between a single and a double bond.²⁴ The cyclohexene ring is pointing away from the Cp^* ligand and has a $\text{C}(14)\text{-C}(15)\text{-W}(1)\text{-N}(1)$ torsion angle of $79.8(5)^\circ$. This orientation is reflective of minimal ligand steric interactions and maximum back-donation of electron density from the metal to the alkene π^* orbitals.^{14,18} In solution, the olefinic carbon ^{13}C NMR resonances of **6** (i.e., δ 39.6 and 40.0) are diagnostic of coordinated alkenes, being shifted upfield by ~ 100 ppm as compared to free cyclohexene.²⁵ A NOE interaction between the methyl H atoms of the Cp^* ring and the olefinic H atoms indicates that the solid-state molecular geometry is maintained in solution.

Complex **6** could conceivably be formed by either associative or dissociative mechanisms from **4a–b**. However, the independent thermolysis of pure **4a** in cyclohexane (70°C , 40 h) merely results in equilibration with **4b**, thus indicating that the pathways to formation of **4a–b** and **6** from **1** are different. It is therefore likely that the C–H activation of cyclohexane by **A** is in direct competition with trapping of **A** by PMe_3 (Scheme 3). The resulting cyclohexyl intermediate undergoes a second C–H activation at the β -H position of the cyclohexyl ring to eliminate neopentane and form a 16e alkene intermediate, which is subsequently trapped by residual PMe_3 to form the 18e adduct **6**. The competitive C–H activation by an unsaturated intermediate in the presence of a strong Lewis base is remarkable, yet it has been observed before²⁶ and is clearly aided by low

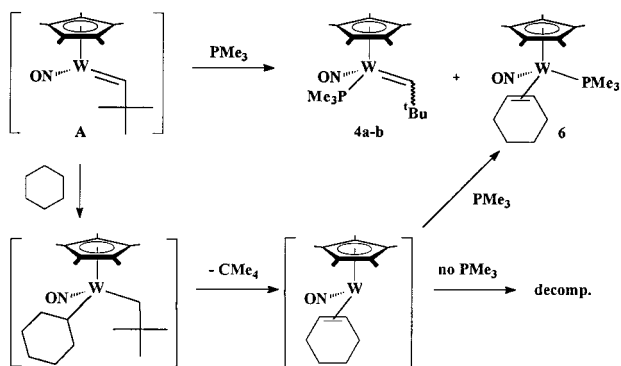
(23) Gladysz, J. A.; Boone, B. J. *Angew. Chem., Intl. Ed. Engl.* **1997**, *36*, 550–583. (b) Kowalczyk, J. J.; Arif, A. M.; Gladysz, J. A. *Chem. Ber.* **1991**, *124*, 729–742.

(24) The strong π -donor ability of the $\text{Cp}^*\text{W}(\text{NO})(\text{PR}_3)$ fragment has been recently demonstrated; see: Burkey, D. J.; Debad, J. D.; Legzdins, P. *J. Am. Chem. Soc.* **1997**, *119*, 1139–1140.

(25) Silverstein, R. M.; Bassler, G. C.; Morrill, T. C. *Spectrometric Identification of Organic Compounds*; Wiley and Sons: Toronto, 1991; p 238.

(26) (a) Buchanan, J. M.; Stryker, J. M.; Bergman, R. G. *J. Am. Chem. Soc.* **1986**, *108*, 1537–1550. (b) McGhee, W. D.; Bergman, R. G. *J. Am. Chem. Soc.* **1988**, *110*, 4246–4262.

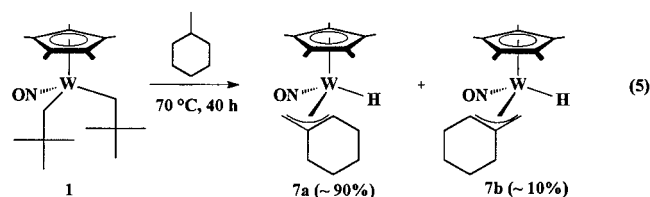
Scheme 3



concentrations of the trapping agent relative to the cyclohexane solvent. The presence of at least 1 equiv of PMe_3 appears to be necessary in order to obtain an isolable organometallic product since the thermolysis of **1** in neat cyclohexane leads to a plethora of intractable Cp^* -containing compounds in the final reaction mixture.

The overall transformation of **1** into **6** can be regarded as involving a functionalization of cyclohexane to cyclohexene by dehydrogenation. The spontaneous dehydrogenation of alkanes to alkenes is not ubiquitous to all metal-based C–H activating systems since the second β -H activation step requires electronic and coordinative unsaturation at the metal center.^{2d} The initial C–H activation event in most systems regenerates a stable, coordinatively saturated complex at which no further chemistry can occur. In our system, however, the resulting C–H activation product is a coordinatively unsaturated 16e species, thereby facilitating multiple C–H activation events.

Activation and Functionalization of Methyl- and Ethylcyclohexane. It is not unreasonable to expect that the thermolysis of **1** in methylcyclohexane under dilute conditions with controlled amounts of PMe_3 should likewise result in the formation of PMe_3 -trapped alkene complexes in relative proportions governed by the selectivity of **A** for primary, secondary, and tertiary sp^3 aliphatic C–H bonds. However, in addition to trace amounts of **4a–b**, the thermolysis of a dilute solution of **1** in methylcyclohexane (6 mM) in the presence of PMe_3 (~10 equiv) unexpectedly yields two products of solvent activation, neither of which contains a phosphine ligand. Specifically, the products are the allyl hydride complexes, $\text{Cp}^*\text{W}(\text{NO})(\eta^3\text{-C}_7\text{H}_{11})(\text{H})$ (**7a–b**) in ~9:1 ratio (eq 5).



Thermolysis of **1** in neat methylcyclohexane produces **7a–b** exclusively. The major product **7a** can be isolated by crystallization from ether/hexanes as yellow needles in reasonable yield (57%). An X-ray crystallographic analysis reveals that **7a** possesses an exocyclic endo, cis- η^3 allyl ligand (Figure 3). The allyl carbon atoms are all within bonding distance of the metal center, while the C–C bond distances are intermediate between double and single bonds. The central allyl carbon is pointing away from, rather than toward, the Cp^* ligand, thereby minimizing steric interactions between the cyclohexyl ring and the Cp^* ligand, while the exocyclic CH_2 group is cis to the

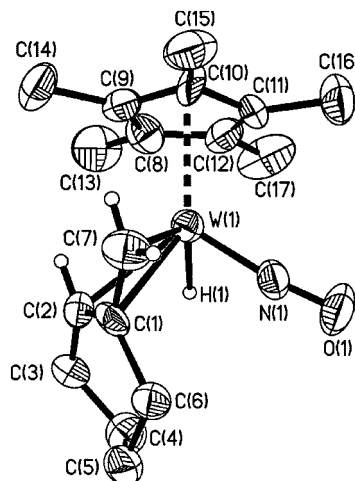


Figure 3. ORTEP plot of the solid-state molecular structure of $\text{Cp}^*\text{W}(\text{NO})(\eta^3\text{-C}_7\text{H}_{11})(\text{H})$ (**7a**) with 50% probability ellipsoids. Selected bond lengths (Å) and angles (deg): $\text{W}(1)\text{--C}(7) = 2.234(11)$, $\text{W}\text{--C}(1) = 2.369(9)$, $\text{W}(1)\text{--C}(2) = 2.397(11)$, $\text{C}(1)\text{--C}(2) = 1.366(14)$, $\text{C}(1)\text{--C}(7) = 1.39(2)$, $\text{C}(2)\text{--C}(1)\text{--C}(7) = 118.7(10)$, $\text{C}(7)\text{--C}(1)\text{--C}(2)\text{--C}(3) = 172.9(11)$, and $\text{N}(1)\text{--W}(1)\text{--C}(1)\text{--C}(6) = -10.9(8)$.

nitrosyl ligand. The allyl ligand is distorted from a conventional η^3 -endo conformation in a manner typical of chiral $\text{Cp}^*\text{M}(\text{NO})\text{L}$ -(allyl) ($\text{M} = \text{Mo}, \text{W}$) complexes.²⁷ It is canted toward the nitrosyl ligand, as indicated by the $\text{N}(1)\text{--W}(1)\text{--C}(1)\text{--C}(6)$ dihedral angle of $-10.9(8)^\circ$. Also, the exocyclic cis $\text{W}\text{--C}$ bond length (2.234(11) Å) is significantly shorter than the other two $\text{W}\text{--C}$ bonds ($\text{W}\text{--C}(1) = 2.369(9)$ Å, $\text{W}\text{--C}(2) = 2.397(11)$ Å), while the $\text{C}(1)\text{--C}(2)$ bond length (1.366(14) Å) is marginally shorter than the $\text{C}(1)\text{--C}(7)$ bond length (1.39(2) Å). Such $\eta^3 \rightarrow \sigma\text{--}\pi$ distortions are believed to be induced by the synergic π -bonding between the mutually perpendicular π -systems of the acceptor NO ligand and the donor π^2 fragment of the allyl ligand.^{18a} The moderate “cis-exocyclic CH_2 ” $\eta^3 \rightarrow \sigma\text{--}\pi$ distortion observed in this instance presumably places the more electron-rich endocyclic π orbitals orthogonal to the NO ligand.

Spectroscopically, complex **7a** exhibits a weak absorption at 1905 cm^{-1} in its Nujol mull IR spectrum in the range expected for terminal $\text{M}\text{--H}$ stretches²⁸ and a hydridic signal in its ^1H NMR (C_6D_6) spectrum. Its ^{13}C NMR spectrum in the same solvent exhibits a high-field, sp^3 -like resonance for the exocyclic allyl carbon (δ 41.3 (t, $^1J_{\text{CH}} = 155\text{ Hz}$)), and low-field, sp^2 -like resonances for the endocyclic allyl carbons (δ 80.0 (d, $^1J_{\text{CH}} = 148\text{ Hz}$), 121.1 (s)), thereby indicating that the $\eta^3 \rightarrow \sigma\text{--}\pi$ distortion of this ligand is maintained in solution. The observation of NOE enhancements between the hydride ligand and the allyl CH atom likewise indicates that the exocyclic CH_2 moiety remains cis to the NO ligand in solution.

The minor product of the thermolysis, **7b**, can be partially characterized by spectroscopic analysis of the final reaction mixture. It exhibits signals in the ^{13}C NMR spectrum consistent with a hydride ligand and a $\eta^3 \rightarrow \sigma\text{--}\pi$ distorted exocyclic allyl ligand. The observation of an NOE enhancement between the allyl CH_2 group and the hydride ligand suggests that complex **7b** is an isomer of **7a** with a trans arrangement of exocyclic

(27) (a) Greenhough, T. J.; Legzdins, P.; Martin, D. T.; Trotter, J. *Inorg. Chem.* **1979**, *11*, 3268–3270. (b) Adams, R. D.; Chodosh, D. F.; Faller, J. W.; Rosan, A. M. *J. Am. Chem. Soc.* **1979**, *101*, 2570–2578. (c) Faller, J. W.; Nguyen, J. T.; Ellis, W.; Mazzieri, M. R. *Organometallics* **1993**, *12*, 1434–1438. (d) Ipaktschi, J.; Mirzaei, F.; Demuth-Eberle, G.; Beck, J.; Serafin, M. *Organometallics* **1997**, *16*, 3965–3972.

(28) Cotton, F. A.; Wilkinson, G.; Murillo, C. A.; Bochmann, M. *Advanced Inorganic Chemistry*, 6th ed.; Wiley & Sons: New York, 1998; pp 79–80.

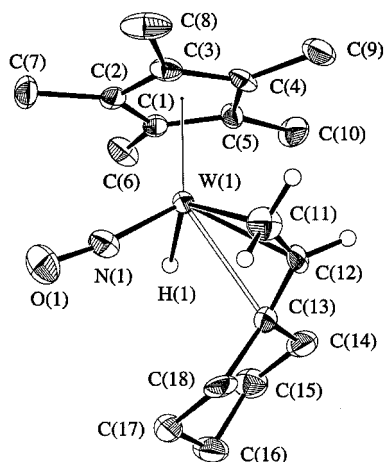
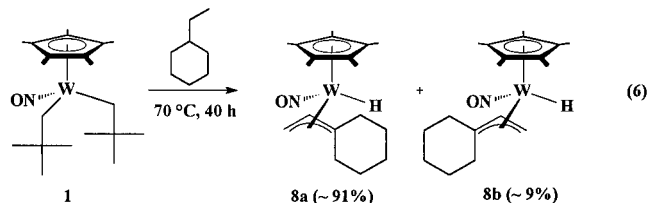


Figure 4. ORTEP plot of the solid-state molecular structure of $\text{Cp}^*\text{W}(\text{NO})(\eta^3\text{-C}_8\text{H}_{13})(\text{H})$ (**8a**) with 50% probability ellipsoids. Selected bond lengths (Å) and angles (deg): $\text{W}(1)\text{-C}(11) = 2.267(8)$, $\text{W}(1)\text{-C}(12) = 2.275(7)$, $\text{W}(1)\text{-C}(13) = 2.476(7)$, $\text{C}(11)\text{-C}(12) = 1.390(11)$, $\text{C}(12)\text{-C}(13) = 1.38(10)$, $\text{C}(11)\text{-C}(12)\text{-C}(13) = 125.7(7)$, and $\text{C}(11)\text{-C}(12)\text{-C}(13)\text{-C}(14) = 173.3(7)$.

CH_2 and NO groups. The exo or endo configuration of **7b** could not be conclusively established by NOE experiments, but given the steric preference for the endo form in **7a**, **7b** is likely the endo, trans isomer. A small amount of spin saturation transfer is observed between the allyl CH atoms of **7a** and **7b** in the NOE difference spectra, thus indicating that **7a** and **7b** interconvert on the NMR time scale at room temperature, likely by rotation around the terminal C–C bond of an unobserved η^1 -allyl intermediate.²⁹

Similar results are obtained for the thermolysis of **1** in neat ethylcyclohexane. Two isomeric allyl hydride complexes, $\text{Cp}^*\text{W}(\text{NO})(\eta^3\text{-C}_8\text{H}_{13})(\text{H})$ (**8a–b**), are detectable in the final thermolysis residue in $\sim 10:1$ ratio (eq 6), and the major isomer



8a can be isolated as a yellow crystalline solid (37% yield).

An X-ray crystallographic analysis of **8a** reveals an exocyclic η^3 -allyl moiety in the exo configuration, again consistent with the complex adopting the conformation that minimizes steric interactions between the Cp^* ligand and the cyclohexyl ring (Figure 4). The allyl ligand is also canted toward the NO ligand with the terminal CH_2 moiety cis to the nitrosyl ligand. Interestingly, the allyl ligand is distorted in a fashion alternative to the $\sigma\text{-}\pi$ distortion extant in **7a**. Both the terminal and the central allyl carbons have short W–C bonds ($\text{W}\text{-C}(11) = 2.267(8)$ Å, $\text{W}\text{-C}(12) = 2.275(7)$ Å) as compared to the endocyclic allyl carbon ($\text{W}\text{-C}(13) = 2.476(7)$ Å). Similar $\eta^3 \rightarrow \eta^2$ distortions have been observed previously in other complexes bearing asymmetric η^3 -allyl ligands, such as the $[\text{TpMo}(\text{NO})(\text{CO})(\eta^3\text{-allyl})]^+$ cations, and they have been attributed to nonbonding steric effects.³⁰ Indeed, the ^{13}C NMR

chemical shifts for the allyl carbons of **8a** in solution are more reminiscent of a terminal $\eta^3 \rightarrow \sigma\text{-}\pi$ distortion (δ 37.2 (t, $^1J_{\text{CH}} = 152$ Hz, allyl CH_2), 93.2 (d, $^1J_{\text{CH}} = 150$ Hz, allyl CH), 109.0 (s, allyl C)), thereby suggesting that the $\eta^3 \rightarrow \eta^2$ distortion may just be a solid-state phenomenon.³¹

The ^1H and ^{13}C NMR spectroscopic properties of the minor product, **8b**, are consistent with it being a terminal allyl isomer of **8a**. NOE enhancements between the terminal CH_2 group and the hydride ligand indicate a trans arrangement of the allyl CH_2 moiety and the nitrosyl ligand, and a small amount of spin saturation transfer can be observed between the respective allyl resonances of **8a** and **8b**. Given the steric preference for the exo over the endo configuration in **8a**, **8b** is probably the exo, trans isomer.

The mechanisms for the transformations of **1** into **7a–b** and **8a–b** likely mirror that of cyclohexane, where the activation of a solvent C–H bond by **A** is followed by β -H activation to release the second neopentyl ligand as neopentane and form a 16e alkene complex. Unlike the cyclohexane case, however, the alkene complex evidently does not persist long enough to be trapped by PMe_3 . Rather, there is a third γ -H activation by the metal center to intramolecularly trap the alkene complex as the 18e allyl hydride complex.³² Formally this represents a triple dehydrogenation, where both the neopentylidene ligand and the metal center function as hydrogen acceptors during the conversion of the alkane to a coordinated allyl. Intriguingly, the allyl ligands of related complexes $[\text{CpM}(\text{NO})(\text{L})(\eta^3\text{-allyl})]^+$ ($\text{M} = \text{Mo}, \text{W}$; $\text{L} = \text{CO}, \text{X}^-, \text{OH}_2$) have been regioselectively, and in some cases stereoselectively, transformed into a wide variety of liberated, functionalized alkenes in high yields by reactions with both nucleophiles and electrophiles.^{27b,c,33} It is therefore conceivable that the allyl hydride complexes that are obtained from C–H activation by **A** will react in the same manner, thereby facilitating the functionalization of the alkanes into complex alkene derivatives.

Selectivity of Alkane C–H Bond Activation by Neopentylidene Complex A. The original purpose of the thermolysis of **1** in methylcyclohexane was to establish the intramolecular selectivity of **A** for aliphatic C–H bonds. The formation of exocyclic allyl hydride complexes in methylcyclohexane and in ethylcyclohexane suggests that initial activation by **A** occurs at the terminal primary methyl C–H bond. The preferential activation of the stronger primary C–H bond would be consistent with the bond selectivities exhibited by all other metal-based systems operating via nonradical mechanisms under both kinetic and thermodynamic control.^{2b,34} However, it is

(31) Spectroscopically, complex **8a** also exhibits a weak terminal W–H stretch at 1935 cm^{-1} in its IR spectrum and a hydride signal at $\delta = 0.92$ ($^1J_{\text{HW}} = 125$) in its ^1H NMR spectrum.

(32) It is curious to note that similar stable allyl hydride complexes are not observed as the final products in the thermolysis of **1** in neat cyclohexane. There are two possible explanations. One is that the third activation does not occur for the endocyclic cyclohexenyl complex, leading to decomposition of the unsaturated 16e species unless trapped by PMe_3 . The other explanation is that the allyl hydride complexes do form by intramolecular trapping but are thermally unstable under the experimental conditions, leading to the observed decomposition products. Attempts to resolve the issue experimentally have so far been unsuccessful. Spectroscopic analysis of the reaction mixtures from the thermolysis of **1** at lower temperatures or at partial conversion do reveal trace amounts of resonances that could be attributable to allyl hydride complexes, but decomposition products dominate the spectra in either case.

(33) (a) Kocienski, P. J.; Brown, R. C. D.; Pommier, A.; Procter, M.; Schmidt, B. *J. Chem. Soc., Perkin Trans. 1* **1998**, *1*, 9–40. (b) Faller, J. W.; Chao, K. *J. Am. Chem. Soc.* **1983**, *105*, 3893–3898. (c) VanArsdale, W. E.; Winter, R. E. K.; Kochi, J. K. *Organometallics* **1986**, *5*, 645–655. (d) Chen, C. C.; Fan, J.; Shieh, S.; Lee, G.; Peng, S.; Wang, S.; Lui, R. *J. Am. Chem. Soc.* **1996**, *118*, 9279–9287. (e) Faller, J. W.; Linebarrier, D. L. *Organometallics* **1990**, *9*, 3182–3184.

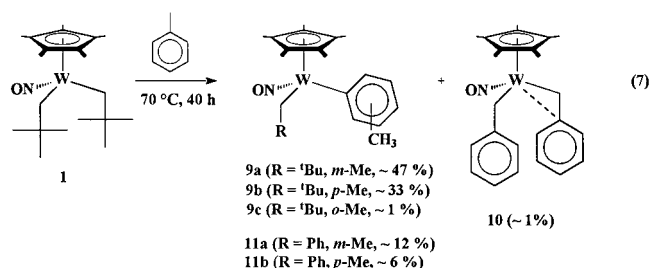
(29) Reference 28; pp 24–25.

(30) (a) Villanueva, L. A.; Ward, Y. D.; Lachicotte, R.; Liebeskind, L. S. *Organometallics* **1996**, *15*, 4190–4200. (b) Ward, Y. D.; Villanueva, L. A.; Allred, G. D.; Payne, S. C.; Semones, M. A.; Liebeskind, L. S. *Organometallics* **1995**, *14*, 4132–4156.

possible that the complexes **7a–b** and **8a–b** arise from initial activation at one of the other allyl positions, followed by dehydrogenation at the methyl position. Alternatively, since the C–H activation steps are all post-rate-determining, other allyl hydride isomers could be derived from activation by **A** at nonallyl endocyclic positions but undergo rapid isomerization (e.g., by reversible γ -H activation) to the more thermodynamically stable isomers **7a–b** and **8a–b**. In other words, the observed product distributions may not be kinetically controlled and therefore may not correlate to the intramolecular selectivity of **A** for alkane C–H bonds. Since no scenario can be discounted at present, the intramolecular C–H bond selectivity of **A** for alkanes cannot conclusively be determined from the activation of these substrates.

C. Activation of Toluene by Neopentylidene Complex **A**.

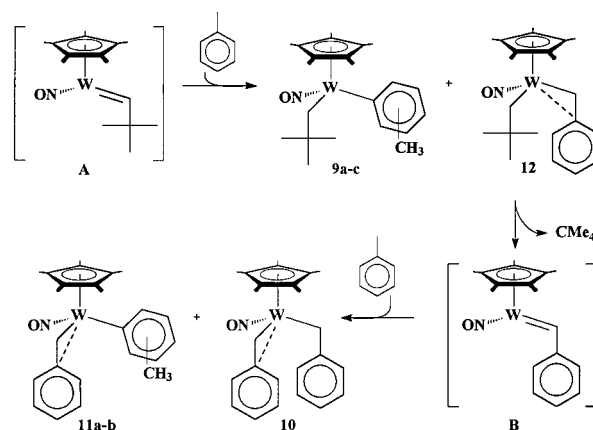
The intramolecular C–H bond selectivity of **A** for arene C–H bonds can, in theory, be deduced from the activation of toluene. Specifically, the relative preference of **A** for aryl sp^2 versus benzylic sp^3 C–H bonds should be reflected in the distribution of aryl and benzylic activated products. Likewise, the regioselectivity of aryl activation (ortho, meta, para) should be reflected in the relative distribution of aryl isomers. The thermolysis of **1** in toluene, however, yields a surprisingly complex mixture of six products (eq 7). The two major products are the



neopentyl aryl complexes, namely, $Cp^*W(NO)(CH_2CMe_3)(C_6H_4-3-Me)$ (**9a**) and the previously reported $Cp^*W(NO)(CH_2CMe_3)(C_6H_4-4-Me)$ ³⁵ (**9b**) in approximately 47 and 33% yields, respectively. Complexes **9a–b** can be isolated in crystalline form as a mixture (56% yield) and are readily distinguished by the distinct aromatic $^3J_{H-H}$ coupling patterns in the 1H NMR spectrum of the mixture. The other spectroscopic features of **9a–b** are unremarkable. The other four products resulting from this thermolysis can be identified from the 1H NMR spectrum of the final reaction mixture. One is the previously reported aryl isomer of **9a–b**, namely $Cp^*W(NO)(CH_2CMe_3)(C_6H_4-2-Me)$ (**9c**;¹² ~1%). The remaining three products all arise from the incorporation of *two* molecules of toluene; namely, $Cp^*W(NO)(CH_2C_6H_5)(C_6H_4-3-Me)$ (**11a**; ~12%), $Cp^*W(NO)(CH_2C_6H_5)(C_6H_4-4-Me)$ (**11b**; ~6%), and the previously reported $Cp^*W(NO)(CH_2C_6H_5)_2$ (**10**;³⁶ ~1%).

Evidence for the Formation of the C–H Activating Benzylidene Complex $Cp^*W(NO)(=CHC_6H_5)$. To determine the origin of products **9–11**, the thermolysis of **1** in toluene at 70 °C was monitored by periodic 1H NMR spectroscopic analysis of the reaction mixture. Over the course of the first 15 h, *all four* products of toluene C–H activation by **A** are observed to form, specifically **9a–c** and the product of activation at the tolyl methyl position, namely, $Cp^*W(NO)(CH_2CMe_3)(CH_2C_6H_5)$

Scheme 4



(**12**). However, **12** disappears as the thermolysis progresses and is replaced by the benzyl-containing products **10** and **11a–b**. This observation suggests that complex **12** is thermally unstable under the experimental conditions employed and mediates the formation of **10** and **11a–b**. In support of this hypothesis is the fact that thermolysis of independently prepared **12** in toluene for 40 h at 70 °C yields **10** and **11a–b** in the same relative distributions as from **1** (i.e., **11a**:**11b**:**10** = 63:32:5). Complex **11a** can be isolated as a crystalline solid from this reaction mixture in adequate yield (25%) and fully characterized, but **11b** can only be further characterized spectroscopically in the crude reaction mixture. Both **11a** and **11b** exhibit spectral features typical of $Cp^*M(NO)(CH_2C_6H_5)(aryl)$ ($M = Mo, W$) complexes, most notably η^2 -benzyl ligands characterized by the ipso carbon resonances at ~114 ppm in their ^{13}C NMR spectra.^{36,37}

The transformation of **12** into **10** and **11a–b** could proceed via any of the mechanisms previously discussed for **1** (vide supra), but the most likely mechanism is the α -H elimination of neopentane from **12** to generate a C–H activating benzylidene complex, **B** (Scheme 4).

The proposed mechanism does have literature precedents. The complex $Cp_2Ti(CH_2C_6H_4-4-Me)_2$ has been obtained from the thermolysis of $Cp_2Ti(CH_2CMe_3)_2$ in *p*-xylene, and the related PMe_3 -trapped intermediate, $Cp_2Ti(=CHC_6H_5)$, has been observed spectroscopically during the thermolysis of $Cp_2Ti(CH_2CMe_3)(CH_2C_6H_5)$.⁹ The mechanism is also supported by the following experimental observations. The thermolysis of **12** in benzene and benzene- d_6 cleanly affords $Cp^*W(NO)(CH_2C_6H_5)(C_6H_5)$ (**13**) and $Cp^*W(NO)(CHDC_6H_5)(C_6D_5)$ (**13- d_6**), respectively, in addition to free neopentane. Complex **13- d_6** exhibits stereospecific syn incorporation of deuterium at the methylene carbon, consistent with concerted 1,2-*cis* addition of C–H across the $M=C$ linkage of an anticlinal benzylidene intermediate. Monitoring the rate of reaction of **12** in benzene by 1H NMR spectroscopy at 72 °C affords a first-order rate constant of the same order of magnitude as **1** (i.e., $k_{12} = 4.9(1) \times 10^{-5} s^{-1}$; $k_{12}/k_1 = 1.07$), thus indicating a similarity in the energetics of the rate-determining steps.

Finally, the thermolysis of **12** in THF in the presence of excess PMe_3 (~130 equiv) results in the clean formation of $Cp^*W(NO)(=CHC_6H_5)(PMe_3)$ **14a–b** in two rotameric forms (~5:1 ratio). The major isomer **14a** is isolable as an orange crystalline solid (52% yield) and has been subjected to an X-ray crystallographic analysis (Figure 5). The solid-state molecular structure of **14a** is similar to that of **4a**, with a short $W=C(1)$

(34) For a detailed discussion of the origin of this phenomenon, see: Bryzndza, H. E.; Fong, L. K.; Paciello, R. A.; Tam, W.; Bercau, J. E. *J. Am. Chem. Soc.* **1987**, *109*, 1444–1456.

(35) Debad, J. D.; Legzdins, P.; Rettig, S. J.; Veltheer, J. E. *Organometallics* **1993**, *12*, 2714–2725.

(36) Legzdins, P.; Jones, R. H.; Phillips, E. C.; Yee, V. C.; Trotter, J.; Einstein, F. W. B. *Organometallics* **1991**, *10*, 986–1002.

(37) Dryden, N. H.; Legzdins, P.; Trotter, J.; Yee, V. C. *Organometallics* **1991**, *10*, 2857–2870.

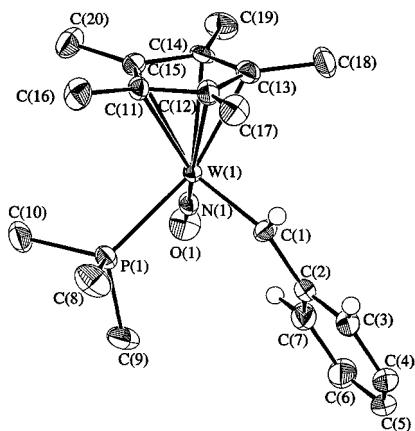


Figure 5. ORTEP plot of the solid-state molecular structure $\text{Cp}^*\text{W}(\text{NO})(=\text{CHC}_6\text{H}_5)(\text{PMe}_3)$ (**14a**) with 50% probability ellipsoids. Selected bond lengths (Å) and angles (deg): $\text{W}(1)\text{--C}(1) = 1.975(3)$, $\text{N}(1)\text{--O}(1) = 1.244(6)$, $\text{W}(1)\text{--N}(1)\text{--O}(1) = 178.1(3)$, $\text{W}(1)\text{--C}(1)\text{--C}(2) = 137.2(2)$, $\text{W}(1)\text{--C}(1)\text{--C}(2)\text{--C}(3) = -171.3(3)$, and $\text{N}(1)\text{--W}(1)\text{--C}(1)\text{--C}(2) = -8.3(4)$.

bond of 1.975(3) Å and a nearly planar $\text{N}(1)\text{--W}(1)\text{--C}(1)\text{--C}(2)$ grouping ($-8.3(4)^\circ$). An additional structural feature is the planar alignment of the phenyl and $\text{W}=\text{C}$ moieties ($\text{W}(1)\text{--C}(1)\text{--C}(2)\text{--C}(3) = 171.3(3)^\circ$), which is indicative of conjugation of the alkylidene and phenyl π -systems.³⁸ In solution, **14a** exhibits diagnostic high-field NMR resonances for the benzyldiene protons (δ 12.01, $^1J_{\text{HP}} = 3.8$ Hz) and the benzyldiene carbon (δ 261.2, $^2J_{\text{CP}} = 9$ Hz). The NOE enhancements between the Cp^* ring and the benzyldiene H atom reveal that the anticlinal orientation of the Cp^* and Ph groups is maintained in solution. Not surprisingly, the spectroscopic features of the minor isomer **14b** are consistent with it being the synclinal geometric isomer. The trapping reaction appears to be irreversible since heating pure **14a** in C_6D_6 (70 °C, 24 h) results in intramolecular isomerization to **14b**, with no evidence for the formation of **13-d**.

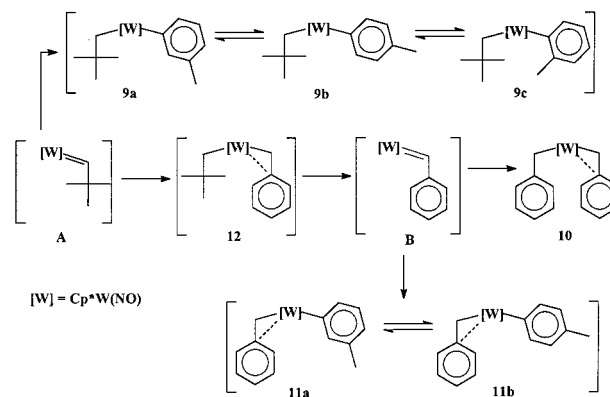
Selectivity of Aryl versus Benzylic C–H Bond Activation by Complexes A and B. Monitoring the thermolysis of **1** in toluene for an additional 24 h past the end point of typical thermolysis experiments (64 h total) reveals no significant changes in the ^1H NMR spectrum.³⁹ This indicates that, once formed, the neopentyl-containing products **9a–c** do not convert to the benzyl-containing products **10** and **11a–b** (e.g., via isomerization to **12**). In addition, the relative ratios of aryl isomers **9a–c** and **11a–b** remain constant during their formation from **1** and **12**, respectively. These results suggest that the product distributions observed after the consumption of **12** (i.e., at 40 h) may indeed be a kinetic distribution of products and thus correlate to the intramolecular C–H bond selectivities of **A** and **B**.

To test this hypothesis, three representative complexes were synthesized by metathetical methods and thermolyzed independently in toluene at 70 °C for 24 h. As anticipated, the bis-(benzyl) complex **10** is thermally robust and does not convert to **11a–b**. Likewise, the neopentyl *o*-tolyl complex **9c** does not convert to the benzyl complexes **10** or **11a–b**. Surprisingly,

(38) For other examples of isostructural benzyldiene complexes, see: (a) Chan, M. C. W.; Cole, J. M.; Gibson, V. C.; Howard, J. A. K.; Lehmann, C.; Poole, A. D.; Siemeling, U. *J. Chem. Soc., Dalton Trans.* **1998**, 103–111. (b) Mashima, K.; Tanaka, Y.; Kaidzu, M.; Nakamura, A. *Organometallics* **1996**, *15*, 2431–2433. (c) Kiel, W. A.; Lin, G.; Constable, A. G.; McCormick, F. B.; Strouse, C. E.; Eisenstein, O.; Gladysz, J. A. *J. Am. Chem. Soc.* **1982**, *104*, 4865–4878.

(39) A trace amount of unidentified decomposition products is observed at 64 h and the amount gradually increases upon prolonged heating.

Scheme 5



however, **9c** does convert quantitatively to the same relative distribution of aryl isomers **9a–c** as observed during the thermolysis of **1** in toluene ($\sim 47:33:1$). The thermolysis of **9c** in benzene- d_6 at 70 °C reveals that the isomerization is a rapid intramolecular process ($t_{1/2} = 18$ min), with **9a** and **9b** forming concomitantly to attain the equilibrium distribution after 120 min.⁴⁰ Similar experiments with the third representative complex, namely, the previously unobserved benzyl *o*-tolyl isomer, $\text{Cp}^*\text{W}(\text{NO})(\text{CH}_2\text{C}_6\text{H}_5)(\text{C}_6\text{H}_4\text{-2-Me})$ (**11c**), also reveal a concomitant intramolecular isomerization to a 2:1 mixture of **11a** and **11b** ($t_{1/2} = 61$ min in benzene- d_6).⁴¹ The rapid isomerizations of both **9c** and **11c** indicate that the relative distributions of aryl-activation isomers **9a–c** and **11a–b** do not represent the regioselectivity of **A** and **B** for the ortho, meta and para aryl bonds of toluene but instead reflect the relative thermodynamic stabilities of the respective aryl complexes. An important consequence of the isomerizations is that unobserved intermediates must be present in solution to mediate the migration of the metal carbon bond of the aryl ligand. Similar cases of aryl isomerizations in other C–H activating systems have been attributed to the reversible formation of π - $3c$ or σ - $4d$ arene complexes, or benzyne complexes,^{4a} via intramolecular H atom transfer. Various such intermediates could be formed in this case by H-transfer from the alkyl and aryl ligands and/or from a methyl group of the Cp^* ligand. Investigations into the mechanism of the isomerization process and its relation to the C–H activation of arenes are currently underway. The relationship between all of the complexes derived from the activation of toluene from **1** is thus shown in Scheme 5.

Fortuitously, the lack of interconversion of the respective aryl and benzylic C–H activation products under thermolytic conditions indicates that the aryl and benzylic C–H bond activation pathways from **A** and **B** are effectively independent and irreversible. In other words, the observed aryl versus benzylic product distributions do in fact reflect the intramolecular kinetic selectivities of **A** and **B** for the aryl sp^2 and benzylic sp^3 C–H bonds in toluene. The respective selectivities of **A** and **B** can also be independently quantified since the ratio of the products **9a–c** to **10** and **11a–b** represents the aryl versus benzylic kinetic selectivity of **A**, while the ratio of **10** to **11a–b** represents that of **B**.⁴² The ratios of 4.3(3):1 for **A** and 19(2):1 for **B** clearly indicate a preferences for activation of the stronger aryl sp^2 C–H bond. Thus, both alkylidene intermediates do, in

(40) No resonances attributable to free toluene, **10**, or **11a–b** are observed, even after prolonged heating for 40 h. Rather, **9a–c** slowly decompose to release free neopentane, presumably via reaction with benzene in the same manner as **5**.

(41) No resonances attributable to free toluene or **10** are observed, even after prolonged heating for 40 h. Rather, **11a–b** slowly decompose to a plethora of unidentified products.

fact, possess the same qualitative bond selectivity as the majority of reported metal-based C–H activation systems.^{2b,43} Furthermore, this fact supports the inference that the activation and functionalization of alkanes such as methylcyclohexane does indeed proceed by initial C–H activation of the stronger primary C–H bond.

The relative intramolecular kinetic selectivities of **A** and **B** can be readily compared to those of other representative complexes that activate toluene by alternative mechanisms under kinetic conditions. Both alkylidene complexes exhibit selectivities that are higher than that exhibited by $\text{Tp}^*\text{Rh}(\text{PMe}_3)$ (3.5:1 at 25 °C) for oxidative addition of tolyl C–H bonds.⁴⁴ They bracket that of Cp^*ScMe (6.1:1 at 80 °C) for σ -bond metathesis of tolyl C–H^{4d} but are considerably less than that exhibited by $\text{Cp}^*\text{Rh}(\text{PMe}_3)$ (>99:1 at –45 °C)⁴⁵ and $\text{Cp}^*\text{Ir}(\text{PMe}_3)$ (>99:1 at 25 °C)⁴⁶ that operate by oxidative–addition mechanisms. Similarly large (99:1 or greater) kinetic selectivities have been reported for the activation of toluene by 1,2 C–H addition to $(\text{HNR})_2\text{Zr}=\text{NR}$ (R = ^tBu₃Si) at 97 °C^{5b} and by C–H addition to photochemically activated $\text{TpRe}(\text{O})(\text{I})(\text{Cl})$ at 25 °C.⁴⁷ Thus, it appears that the intramolecular kinetic selectivities of alkylidene complexes **A** and **B** for arene C–H bonds are modest at best. In comparison to each other, however, **B** appears to be significantly more selective than **A**, thereby indicating that the alkylidene R substituent can influence the C–H activation process.

D. Activation of Aliphatic C–H Bonds by Benzylidene Complex B. The C–H activation ability of the benzylidene complex **B** encompasses aliphatic substrates as well. Thus, the thermolysis of **12** in neat tetramethylsilane at 70 °C for 40 h cleanly yields the previously reported $\text{Cp}^*\text{W}(\text{NO})(\text{CH}_2\text{C}_6\text{H}_5)(\text{CH}_2\text{SiMe}_3)$ (**15**);³⁷ ~95% as judged by ¹H NMR spectroscopy) via primary sp³ C–H bond activation. Likewise, the thermolysis of **12** in cyclohexane in the presence of PMe_3 (~10 equiv) generates **6** via secondary sp³ C–H bond activation, in addition to the alkylidene complexes **14a–b**. Finally, the thermolysis of **12** in methylcyclohexane and ethylcyclohexane forms the same distributions of allyl hydride complexes **7a–b** and **8a–b** as observed during the corresponding thermolyses of **1**. These results clearly indicate that **B** is as effective as **A** in activating the various types of C–H bonds of both alkane and arene substrates. This is in sharp contrast to the related $\text{Cp}_2\text{Ti}=\text{NR}$ system, where the replacement of an alkyl R substituent with an aryl substituent renders the complex unreactive toward hydrocarbons.^{5f} The confirmed activation of alkanes by **B** also supports the notion that a third alkylidene complex, namely, $\text{Cp}^*\text{W}(\text{NO})(=\text{CHSiMe}_3)$, likely mediates the observed slow conversion of $\text{Cp}^*\text{W}(\text{NO})(\text{CH}_2\text{CMe}_3)(\text{CH}_2\text{SiMe}_3)$ (**2**) to $\text{Cp}^*\text{W}(\text{NO})(\text{CH}_2\text{SiMe}_3)_2$ (**3**) by aliphatic C–H bond activation of tetramethylsilane (eq 1).

Epilogue

Our initial exploration of the thermal chemistry of **1** and **12** has uncovered several important characteristics of C–H bond

(42) Calculation for **A**: (**9a–c**):(**10** and **11a–b**) = (46 + 34 + 1):(19) or 4.3(3):1. Calculation for **B**: (**11a–b**):**10** = 63 + 32:5 or 19(2), with an error of 7% in the relative integrations of aryl and benzylic products.

(43) For a detailed discussion on the origin of this kinetic selectivity for C–H activation by a 1,2 concerted R–H addition process, see refs 5b,c.

(44) Jones, W. D.; Hessel, E. T. *J. Am. Chem. Soc.* **1993**, *115*, 554–562.

(45) Jones, W. D.; Feher, F. J. *J. Am. Chem. Soc.* **1984**, *106*, 1650–1663.

(46) Burger, P.; Bergman, R. G. *J. Am. Chem. Soc.* **1993**, *115*, 10462–10463.

(47) Brown, S. N.; Myers, A. W.; Fulton, J. R.; Mayer, J. M. *Organometallics* **1998**, *17*, 3364–3374.

activation by the alkylidene complexes **A** and **B** that reveal them to be versatile and useful additions to this area of synthetic chemistry. First, the activation of C–H bonds occurs via the 1,2-R–H addition to the W=C double bond of one alkylidene isomer, with a modest kinetic preference for the strongest C–H bond. Second, spontaneous functionalization can be effected for alkane substrates due to the inherent unsaturated, 16e nature of the resulting C–H activation products. In particular, alkylcyclohexanes are converted to allyl ligands that have the potential for further elaboration and liberation as functionalized alkenes. Finally, the C–H activating ability of $\text{Cp}^*\text{W}(\text{NO})(=\text{CHR})$ intermediates appears to be quite general as alkylidenes **A** (R = ^tBu), **B** (R = Ph), and possibly **C** (R = SiMe₃) activate alkane and arene C–H bonds. Presumably then, α -H elimination of neopentane by the thermolysis of other congeners of the large family of available $\text{Cp}^*\text{W}(\text{NO})(\text{CH}_2\text{CMe}_3)(\text{CH}_2\text{R})$ complexes can provide a whole host of alkylidene complexes for exploitation as alkane functionalization reagents. Our studies with these and related alkylidene complexes designed to address the features outlined above are currently in progress.

Experimental Section

General Methods. All reactions and subsequent manipulations involving organometallic reagents were performed under anaerobic and anhydrous conditions under either high vacuum or an atmosphere of prepurified argon or dinitrogen. General procedures routinely employed in these laboratories have been described in detail elsewhere.⁴⁸ Unless otherwise specified, all reagents were purchased from commercial suppliers and used as received. Hydrocarbon solvents and trimethylphosphine were freshly distilled or vacuum transferred from sodium or sodium/benzophenone ketyl. Tetrahydrofuran was distilled from molten potassium. Tetramethylsilane-*d*₁₂ (99.8%, CDN Isotopes), benzene-*d*₆, and dioxane-*d*₈ were dried over sodium and vacuum-transferred as required. Methylene chloride-*d*₂ and chloroform-*d*₁ were dried over activated 4-Å molecular sieves and vacuum-transferred as required. The $\text{R}_2\text{Mg}\cdot\text{X}(\text{dioxane})$ (R = CX₂CMe₃ (X = H, D), CH₂C₆H₅, C₆H₄-2-Me) alkylating reagents^{17,49} and the complexes $\text{Cp}^*\text{W}(\text{NO})(\text{R})(\text{R}')$ (R = CH₂CMe₃, R' = CH₂CMe₃, CH₂C₆H₅, C₆H₄-2-Me; R = R' = CD₂CMe₃;^{2,35} R = CH₂C₆H₅, R' = C₆H₄-2-Me)³⁷ were prepared according to published procedures. Pertinent synthetic details and characterization data for the new compounds $\text{Cp}^*\text{W}(\text{NO})(\text{CH}_2\text{C}_6\text{H}_5)(\text{C}_6\text{H}_4\text{-2-Me})$ (**11c**) and $\text{Cp}^*\text{W}(\text{NO})(\text{CH}_2\text{C}_6\text{H}_5)(\text{CH}_2\text{CMe}_3)$ (**12**) are reported below.

All IR samples were prepared as Nujol mulls sandwiched between NaCl plates. NMR spectra were recorded at room temperature on Bruker AC 200, Varian XL 300, Bruker WH-400 or Bruker AMX 500 instruments. All chemical shifts are reported in ppm and all coupling constants are reported in hertz. ¹H NMR spectra are referenced to the residual protioisotopomer present in a particular solvent. ¹³C NMR spectra are referenced to the natural-abundance carbon signal of the solvent employed. ²H and ³¹P NMR spectra are referenced to external C₆H₅D (7.15 ppm) and P(OMe)₃ in C₆D₆ (141.0 ppm), respectively. Where appropriate, ¹H–¹H COSY, ¹H–¹H NOEDS, ¹H–¹³C HMQC, ¹H–¹³C HMBC, ¹³C APT, homonuclear decoupling, and gated ¹³C{¹H} experiments were carried out to correlate and assign ¹H and ¹³C signals.

Thermolyses of 1 and 12: The preparation of **2–11** and **13–15** by thermolyses of **1** or **12** was performed in a similar manner unless otherwise stated. The thermolysis of **1** in tetramethylsilane is described below as a representative example. Major products were isolated by crystallization from the final thermolysis mixture using appropriate solvents. The reported yields are not optimized. Minor products that could not be isolated were characterized spectroscopically from the final reaction mixture. Average product ratios were obtained by

(48) Legzdins, P.; Rettig, S. J.; Ross, K. J.; Batchelor, R. J.; Einstein, F. W. B. *Organometallics* **1995**, *14*, 5579.

(49) Dryden, N. H.; Legzdins, P.; Rettig, S. J.; Veltheer, J. E. *Organometallics* **1992**, *11*, 2583–2590.

integration of appropriate signals in the ^1H NMR spectrum of the final reaction mixture. Typically, the standard deviations in the averages were <7%.

Cp*W(NO)(CH₂CMe₃)(CH₂SiMe₃) (2). In the glovebox, a thick-walled reaction bomb was charged with **1** (48 mg, 0.098 mmol) and a stir bar. On a vacuum line, tetramethylsilane (~4 mL) was added via vacuum transfer at $-196\text{ }^\circ\text{C}$. The resulting ruby-red solution was allowed to warm to room temperature and then was placed in an oil bath set at $70(2)\text{ }^\circ\text{C}$ for 40 h. During this time, the solution darkened to wine-red. The organic volatiles were removed under vacuum, and the residual purple-red solid was dissolved in C₆D₆ and analyzed by ^1H NMR spectroscopy. The NMR solvent was removed in vacuo, and the residue was dissolved in pentane and filtered through Celite (1 × 0.7 cm) supported on a frit. The filtrate was reduced in volume and stored at $-30\text{ }^\circ\text{C}$ for several days to induce the deposition of **2** (45 mg, 90%) as maroon crystals. The characterization data for this complex match that previously reported:³⁵ IR (cm⁻¹) 1551 (s, ν_{NO}); ^1H NMR (400 MHz, C₆D₆) δ -2.10 (dd, $^2J_{\text{HH}} = 12.8$, $^4J_{\text{HH}} = 1.9$, 1H, CH_{syn}HCM₃), -1.35 (dd, $^2J_{\text{HH}} = 12.0$, $^4J_{\text{HH}} = 2.2$, 1H, CH_{syn}HSiMe₃), 0.40 (s, 9H, SiMe₃), 1.08 (d, $^2J_{\text{HH}} = 12.0$, 1H, CH_{anti}HSiMe₃), 1.35 (s, 9H, CMe₃), 1.51 (s, 15H, C₅Me₅), 3.25 (d, $^2J_{\text{HH}} = 12.8$, 1H, CH_{anti}HCM₃); NOEDS (400 MHz, C₆D₆) δ irradi at -2.10 ppm, NOEs at δ -1.35, 3.25; irradi at -1.35, NOEs at δ -2.10, 1.08; irradi at 0.40 ppm, NOE at δ -1.35; irradi at 1.08 ppm, NOE at δ -1.35; irradi at 1.35 ppm, NOEs at δ -2.10, 0.40, 3.25; irradi at 3.25 ppm, NOEs at δ -2.10, 1.35.

Cp*W(NO)(CHDCMe₃)(CD₂Si(CD₃)₃) (2-d₁₂). Complex **2-d₁₂** was prepared and analyzed by thermolysis of **1** in tetramethylsilane-*d*₁₂ in a J. Young NMR tube. It was subsequently isolated as mauve crystals by crystallization from pentane (27 mg, 93%); IR (cm⁻¹) 1554 (s, ν_{NO}); MS (LREI, *m/z*, probe temperature $150\text{ }^\circ\text{C}$) 519 [P⁺, ¹⁸⁴W]; ^1H NMR (300 MHz, C₆D₆) δ 1.36 (s, 9H, CMe₃), 1.51 (s, 15H, C₅Me₅), 3.19 (br s, 1H, CH_{anti}D), $^2\text{H}\{^1\text{H}\}$ NMR (77 MHz, C₆H₆) δ -2.16 (s, 1D, CHD_{syn}CM₃), -1.38 (s, 1D, CD_{syn}DSi Me₃), 0.33 (s, 9D, Si(CD₃)₃), 1.06 (s, 1D, CD_{anti}DSiMe₃). Anal. Calcd for C₁₉H₂₅D₁₂NOSiW:⁵⁰ C, 43.94; H/D, 7.13; N, 2.70. Found: C, 44.26; H/D, 7.09; N, 2.74.

Cp*W(NO)(=CHCMe₃)(PMe₃) (4a–b). Complexes **4a–b** were prepared by the thermolysis of **1** (172 mg, 0.350 mmol) in trimethylphosphine (2 mL). Complex **4a** was isolated as platelike yellow crystals (130 mg, 75% yield) by crystallization from Et₂O.

4a: IR (cm⁻¹) 1513 (s, ν_{NO}); MS (LREI, *m/z*, probe temperature $200\text{ }^\circ\text{C}$) 495 [P⁺, ¹⁸⁴W]; ^1H NMR (400 MHz, C₆D₆) δ 1.06 (d, $^2J_{\text{HP}} = 9.0$ Hz, 9H, PMe₃), 1.43 (s, 9H, CMe₃), 1.87 (s, 15H, C₅Me₅), 11.25 (d, $^3J_{\text{HP}} = 3.6$ Hz, 1H, W=CH); ^{13}C NMR (75, MHz, C₆D₆) δ 11.0 (C₅Me₅), 19.7 (d, $^1J_{\text{CP}} = 32.4$ Hz, PMe₃), 32.0 (CMe₃), 52.2 (CMe₃), 106.4 (C₅Me₅), 282.8 (d, $^2J_{\text{CP}} = 8.9$ Hz, W=CH); ^{31}P NMR (121 MHz, C₆D₆) δ -7.9 (s, $^1J_{\text{PW}} = 446$ Hz). NOEDS (400 MHz, C₆D₆) δ irradi at 1.06, NOE at 11.25; irradi at 1.43; NOEs at 1.06, 11.25; irradi at 1.87, NOE at 11.25. Anal. Calcd for C₁₈H₃₄NOPW: C, 43.65; H, 6.92; N, 2.83. Found: C, 43.62; H, 7.00; N, 2.78.

4b: ^1H NMR (400 MHz, C₆D₆) δ 1.14 (d, $^2J_{\text{HP}} = 9.4$ Hz, 9H, PMe₃), 1.15 (s, 9H, CMe₃), 1.97 (s, 15H, C₅Me₅), 12.87 (d, $^3J_{\text{HP}} = 4.4$ Hz, 1H, W=CH); ^{13}C NMR (75, MHz, C₆D₆) δ 11.5 (C₅Me₅), 20.2 (d, $^1J_{\text{CP}} = 31.2$ Hz, PMe₃), 31.9 (CMe₃), 48.3 (CMe₃), 106.6 (C₅Me₅), 282.9 (d, $^2J_{\text{CP}} = 9.5$ Hz, W=CH); ^{31}P NMR (121 MHz, C₆D₆) δ -4.0 (s). NOEDS (400 MHz, C₆D₆) δ irradi at 1.14, NOE at 12.87; irradi at 1.97, NOE at 1.15.

Cp*W(NO)(CH₂CMe₃)(C₆H₅) (5) and Cp*W(NO)(CHDCMe₃)(C₆D₅) (5-d₆). Compounds **5** and **5-d₆** were prepared from the thermolysis of **1** in benzene and benzene-*d*₆, respectively, and isolated as wine-red rods by recrystallization from pentane. The characterization data for complex **5** matched that previously reported.¹²

5: 22 mg (33%); ^1H NMR (300 MHz, C₆D₆) δ -2.05 (d, $^2J_{\text{HH}} = 11.4$, 1H, CH_{syn}H), 1.26 (s, 9H, CMe₃), 1.53 (s, 15H, C₅Me₅), 4.50 (d, $^2J_{\text{HH}} = 11.4$, 1H, CH_{anti}H), 7.10 (m, 3H, Ar H), 7.70 (d, $^3J_{\text{HH}} = 6.0$, 2H, Ar H).

5-d₆: 46 mg (65%); IR (cm⁻¹) 1549 (s, ν_{NO}); MS (LREI, *m/z*, probe temperature $150\text{ }^\circ\text{C}$) 503 [P⁺, ¹⁸⁴W]; ^1H NMR (400 MHz, C₆D₆) δ

1.26 (s, 9H, CMe₃), 1.54 (s, 15H, C₅Me₅), 4.37 (s, 1H, CHD); $^2\text{H}\{^1\text{H}\}$ NMR (77 MHz, C₆H₆) δ -1.95 (br s, CHD), 7.26, 7.55, 7.79 (br m, Ar D). Anal. Calcd for C₂₁H₂₅D₆NOW:⁵⁰ C, 50.12; H/D, 6.22, N, 2.82. Found: C, 50.17; H/D, 6.32; N, 2.78.

Cp*W(NO)(cyclohexene)(PMe₃) (6). Complex **6** was prepared by the thermolysis of **1** (81 mg, 0.16 mmol) in cyclohexane (8 mL) and PMe₃ (~1.6 mmol, ~10 equiv). It was isolated as pale yellow needles (32 mg, 38% yield) by extraction into 4:1 Et₂O/hexanes and filtration through neutral alumina I (1 × 0.7 cm): IR (cm⁻¹) 1518 (s, ν_{NO}); MS (LREI, *m/z*, probe temperature $150\text{ }^\circ\text{C}$) 507 [P⁺, ¹⁸⁴W], 425 [P⁺ - C₆H₁₀]; ^1H NMR (500 MHz, C₆D₆) δ 0.8 (m, 1H, α' CH), 1.22 (d, $^2J_{\text{HP}} = 9\text{H}$, PMe₃), 1.5 (m, 1H, α CH), 1.6 (m, 2H, γ' CHH), 1.67 (s, 15H, C₅Me₅), 1.8 (m, 2H, γ CHH), 2.4 (m, 1H, β' CHH), 2.8 (m, 2H, β CHH), 3.1 (m, 1H, β'' CHH); $^{13}\text{C}\{^1\text{H}\}$ NMR (125 MHz, C₆D₆) δ 10.3 (C₅Me₅), 17.4 (d, $^2J_{\text{CP}} = 29$, PMe₃), 24.2 (γ CH₂), 25.3 (γ' CH₂), 28.3 (β CH₂), 30.8 (d, $^3J_{\text{CP}} = 4$, β' CH₂), 39.6 ($^1J_{\text{CW}} = 39$, α CH), 40.0 (d, $^2J_{\text{CP}} = 12$, α' CH), 103.0 (C₅Me₅); $^{31}\text{P}\{^1\text{H}\}$ NMR (202 MHz, C₆D₆) δ -13.2 (s, $^1J_{\text{PW}} = 373$). Anal. Calcd for C₁₉H₃₄NOPW: C, 44.98; H, 6.76; N, 2.76. Found: C, 44.64; H, 6.77; N, 2.59.

Cp*W(NO)(η^3 -C₇H₁₁)(H) (7a–b). Compounds **7a–b** were prepared from the thermolysis of **1** in methylcyclohexane. Complex **7a** was isolated as yellow needles (28 mg, 70%) by crystallization from pentane.

7a: IR (cm⁻¹) 1905 (w, ν_{WH}), 1564 (s, ν_{NO}); MS (LREI, *m/z*, probe temperature $150\text{ }^\circ\text{C}$) 445 [P⁺, ¹⁸⁴W]; ^1H NMR (400 MHz, C₆D₆) δ -0.73 (s, $^1J_{\text{HW}} = 123$, 1H, WH), 0.31 (br s, 1H, allyl CH_{syn}H), 1.39 (m, 1H, C_bHH), 1.54 (m, 1H, C_aHH), 1.71 (m, 1H, C_bHH), 1.76 (s, 15H, C₅Me₅), 1.84 (m, 1H, C_aHH), 2.28 (br s, 1H, allyl CH), 2.60 (m, 1H, allyl CH_{anti}H), 2.68 (m, 2H, C_cHH, C_dHH), 2.91 (q, 1H, $^2J_{\text{HH}} = 7.9$, C_cHH), 2.97 (m, 1H, C_dHH); $^{13}\text{C}\{^1\text{H}\}$ (75 MHz, C₆D₆) δ 10.7 (C₅Me₅), 22.1 (t, $^1J_{\text{CH}} = 124$, C_aH₂), 22.5 (t, $^1J_{\text{CH}} = 126$, C_bH₂), 28.8 (t, $^1J_{\text{CH}} = 125$, C_cH₂), 29.6 (t, $^1J_{\text{CH}} = 126$, C_dH₂), 41.3 (t, $^1J_{\text{CH}} = 155$, allyl CH₂), 80.0 (d, $^1J_{\text{CH}} = 148$, allyl CH), 104.9 (C₅Me₅), 121.1 (s, allyl C). NOEDS (400 MHz, C₆D₆) δ irradi at -0.73, NOEs at 2.28, 2.97; irradi at 0.31, NOEs at 2.28, 2.68; irradi at 2.28, NOEs at -0.73, 0.31, 2.97; irradi at 2.68, NOE at 0.31. Anal. Calcd. for C₁₇H₂₇NOW: C, 45.86; H, 6.11; N, 3.15. Found: C, 45.99; H, 6.19; N, 2.97.

7b: ^1H NMR (400 MHz, C₆D₆) δ -0.73 (s, 1H, WH), 0.48 (br s, 1H, allyl CHH), 1.75 (s, 15H, C₅Me₅), 2.61 (br s, 1H, allyl CH), 3.95 (m, 1H, allyl CHH), other resonances obscured; $^{13}\text{C}\{^1\text{H}\}$ (75 MHz, C₆D₆) δ 10.3 (C₅Me₅), 22.5, 23.0, 27.3, 29.6 (CH₂), 49.7 (t, $^1J_{\text{CH}} = 155$, allyl CH₂), 62.8 (d, $^1J_{\text{CH}} = 146$, allyl CH), 104.7 (C₅Me₅). The ^{13}C resonance attributable to allyl C was not observed. NOEDS (400 MHz, C₆D₆) δ irradi at 3.95, NOEs at -0.73, 0.48.

Cp*W(NO)(η^3 -C₈H₁₃)(H) (8a–b). Compounds **8a–b** were prepared from the thermolysis of **1** in ethylcyclohexane. Complex **8a** was isolated as yellow needles (21 mg, 37%) by crystallization from pentane.

8a: IR (cm⁻¹) 1935 (m, ν_{WH}), 1575 (s, ν_{NO}); MS (LREI, *m/z*, probe temperature $150\text{ }^\circ\text{C}$) 457 [P⁺ - H₂, ¹⁸⁴W]; ^1H NMR (400 MHz, C₆D₆) δ -0.92 (s, $^1J_{\text{HW}} = 125$, 1H, WH), 1.42 (m, 1H, C_bHH), 1.58 (m, 3H, C_aHH, C_cHH), 1.71 (s, 15H, C₅Me₅), 1.79 (m, 1H, C_bHH), 1.90 (m, 1H, C_dHH), 2.00 (m, 1H, C_cHH), 2.15 (m, 3H, C_dHH, allyl CH_{syn}H, C_eHH), 2.44 (dd, 1H, $^2J_{\text{HH}} = 3.1$, $^3J_{\text{HH}} = 13.3$, allyl CH_{anti}H), 2.51 (m, 1H, C_eHH), 2.66 (dd, $^3J_{\text{HH}} = 7.8$, $^3J_{\text{HH}} = 13.3$, 1H, allyl CH); $^{13}\text{C}\{^1\text{H}\}$ (75 MHz, C₆D₆) δ 10.7 (C₅Me₅), 27.1 (t, $^1J_{\text{CH}} = 132$, CH₂), 30.6 (t, $^1J_{\text{CH}} = 128$, CH₂), 32.6 (t, $^1J_{\text{CH}} = 130$, CH₂), 35.1 (t, $^1J_{\text{CH}} = 126$, CH₂), 37.2 (t, $^1J_{\text{CH}} = 152$, allyl CH₂), 41.0 (t, $^1J_{\text{CH}} = 129$, CH₂), 93.2 (d, $^1J_{\text{CH}} = 150$, allyl CH), 103.8 (C₅Me₅), 109.0 (allyl C). NOEDS (400 MHz, C₆D₆) δ irradi at -0.92 ppm, NOEs at 2.00, 2.15, 2.51; irradi at 2.44 ppm, NOE at 2.15; irradi at 2.66 ppm, NOE at 2.15. Anal. Calcd for C₁₈H₂₉NOW: C, 47.07; H, 6.36; N, 3.05. Found: C, 46.86; H, 6.42; N, 2.96.

8b: ^1H NMR (400 MHz, C₆D₆) δ -0.71 (s, $^1J_{\text{WH}} = 126$, 1H, WH), 0.60 (dd, $^3J_{\text{HH}} = 11.7$, $^2J_{\text{HH}} = 3.5$, 1H, allyl CH_{anti}H), 1.76 (s, 15H, C₅Me₅), 2.87 (dd, $^2J_{\text{HH}} = 3.5$, $^3J_{\text{HH}} = 7.4$, 1H, allyl CH_{syn}H), 4.69 (dd, $^3J_{\text{HH}} = 11.7$, $^3J_{\text{HH}} = 7.4$, 1H, allyl CH), other resonances obscured; $^{13}\text{C}\{^1\text{H}\}$ (75 MHz, C₆D₆) δ 10.5 (C₅Me₅), 27.0 (CH₂), 30.5 (CH₂), 32.5 (CH₂), 33.0 (CH₂), 40.9 (allyl CH₂), 42.8 (CH₂), 100.9 (d, $^1J_{\text{CH}} = 151$, allyl CH), 104.8 (C₅Me₅). The ^{13}C resonance attributable to allyl C was not observed. NOEDS (400 MHz, C₆D₆) δ irradi at 2.87, NOEs at -0.71, 0.60, 4.69; irradi at 0.60 ppm, NOE at 2.87; irradi at 4.69 ppm, NOE at 2.87.

(50) Since the detection method used in the elemental analysis cannot distinguish between D₂O and H₂O, H/D abundances were calculated using $1\text{ D} = 1\text{ H}$.

Cp*W(NO)(CH₂CMe₃)(C₆H₄-3-Me) (9a) and Cp*W(NO)(CH₂CMe₃)(C₆H₄-4-Me) (9b). Complexes **9a** and **9b** were prepared by thermolysis of **1** in toluene and recrystallized as mauve microcrystals (35 mg, 56%) by recrystallization from pentane. The characterization data for **9b** match that previously reported.³⁵ IR (cm⁻¹) 1549 (s, ν_{NO}); MS (LREI, *m/z*, probe temperature 150 °C) 511 [P⁺, ¹⁸⁴W]; ¹H NMR (400 MHz, C₆D₆) **9a**: δ -1.91 (d, ²J_{HH} = 11.7, 1H, CH_{syn}H), 1.26 (s, 9H, CMe₃), 1.56 (s, 15H, C₅Me₅), 2.17 (s, 3H, Tol Me), 4.44 (d, ²J_{HH} = 11.7, 1H, CH_{anti}H), 6.93 (d, ³J_{HH} = 7.4, 1H, Tol H), 7.16 (t, ³J_{HH} = 7.6, 1H, Tol H_{meta}), 7.45 (d, ³J_{HH} = 7.5, 1H, Ar H), 7.76 (s, 1H, Ar H_{ortho}). **9b**: δ -1.83 (d, ²J_{HH} = 11.7, 1H, CH_{syn}H), 1.27 (s, 9H, CMe₃), 1.58 (s, 15H, C₅Me₅), 2.09 (s, 3H, Tol Me), 4.28 (d, ²J_{HH} = 11.7, 1H, CH_{anti}H), 7.03 (d, ³J_{HH} = 7.4, 2H, Tol H); 7.71 (d, ³J_{HH} = 7.4, 2H, Tol H); ¹³C{¹H} NMR (125 MHz, dioxane-*d*₈) **9a**: δ 10.1 (C₅Me₅), 21.4 (Tol Me), 33.9 (CMe₃), 41.3 (CMe₃), 111.45 (C₅Me₅), 121.0 (CH₂), 127.7, 128.8, 137.2, 137.3 (Tol C_{aryl}), 182.9 (Tol C_{ipso}). **9b**: δ 10.0 (C₅Me₅), 21.5 (Tol Me), 33.9 (CMe₃), 41.0 (CMe₃), 111.4 (C₅Me₅), 118.6 (CH₂), 128.6, 133.6, 137.6 (Tol C_{aryl}), 180.2 (Tol C_{ipso}). Anal. Calcd for C₂₂H₃₃NOW: C, 51.67; H, 6.50; N, 2.74. Found: C, 51.78; H, 6.68; N, 2.68.

Cp*W(NO)(CH₂C₆H₅)(C₆H₄-3-Me) (11a) and Cp*W(NO)(CH₂C₆H₅)(C₆H₄-4-Me) (11b). Complexes **11a–b** were prepared by thermolysis of **12** in toluene. Complex **11a** was crystallized as orange microcrystals (19 mg, 25%) by crystallization from 4:1 Et₂O/hexanes.

11a: IR (cm⁻¹) 1562 (s, ν_{NO}); MS (LREI, *m/z*, probe temperature 150 °C) 531 [P⁺, ¹⁸⁴W], 501 [P⁺-NO]; ¹H NMR (400 MHz, C₆D₆) δ 1.59 (s, 15H, C₅Me₅), 2.19 (d, ²J_{HH} = 5.9, 1H, CH_{syn}H), 2.20 (s, 3H, Tol Me), 3.46 (d, ²J_{HH} = 5.9, 1H, CH_{anti}H), 6.56 (t, ³J_{HH} = 7.8, 2H, Bzl H_{meta}), 6.82 (d, ³J_{HH} = 7.1, 1H, Tol H), 6.89 (d, ³J_{HH} = 7.4, 2H, Bzl H_{ortho}), 6.96 (d, ³J_{HH} = 7.1, 1H, Tol H), 7.03 (t, ³J_{HH} = 7.1, 1H, Tol H_{meta}), 7.10 (t, ³J_{HH} = 7.4, 1H, Bzl H_{para}), 7.19 (s, 1H, Tol H_{ortho}); ¹³C{¹H} NMR (75 MHz, CDCl₃) δ 10.60 (C₅Me₅), 20.79 (Tol Me), 48.18 (CH₂), 108.95 (C₅Me₅), 113.57 (Bzl C_{ipso}), 129.11, 132.07, 135.71 (Bzl C_{aryl}), 125.05, 126.67, 128.25, 135.37, 138.7 (Tol C_{aryl}), 172.4 (Tol C_{ipso}). Anal. Calcd for C₂₄H₂₉NOW: C, 54.25; H, 5.50; N, 2.64. Found: C, 54.34; H, 5.65; N, 2.70.

11b: ¹H NMR (400 MHz, C₆D₆) δ 1.60 (s, 15H, C₅Me₅), 2.19 (d, ²J_{HH} = 5.9, 1H, CH_{syn}H), 2.23 (s, 3H, Tol Me), 3.46 (d, ²J_{HH} = 5.9, 1H, CH_{anti}H), 6.58 (t, ³J_{HH} = 7.8, 2H, Bzl H_{meta}), 6.90 (d, ³J_{HH} = 7.4, 2H, Bzl H_{ortho}), 6.92 (d, ³J_{HH} = 7.1, 2H, Tol H), 7.00 (d, ³J_{HH} = 7.1, 2H, Tol H), 7.10 (t, ³J_{HH} = 7.4, 1H, Bzl H_{para}); ¹³C{¹H} NMR (75 MHz, CDCl₃) δ 10.68 (C₅Me₅), 21.26 (Tol Me), 48.22 (CH₂), 108.95 (C₅Me₅), 113.59 (Bzl C_{ipso}), 129.22, 132.09, 135.98 (Bzl C_{aryl}), 128.08, 133.35, 139.2, (Tol C_{aryl}), 168.4 (Tol C_{ipso}).

Cp*W(NO)(CH₂C₆H₅)(C₆H₄-2-Me) (11c). Complex **11c** was prepared via the reaction of Cp*W(NO)(CH₂C₆H₅)Cl (0.160 g, 0.34 mmol) and (2-Me-C₆H₄CH₂)₂Mg·x(dioxane) (0.063 g, 0.34 mmol) in THF (10 mL). The crude residue was extracted with 4:1 Et₂O/hexanes (3 × 5 mL) and filtered through Celite (1 × 0.7 cm) supported on a frit. Concentrating the solution followed by storage at -30 °C overnight provided **11c** as red blocks (55 mg, 32%): IR (cm⁻¹) 1552 (s, ν_{NO}); MS (LREI, *m/z*, probe temperature 150 °C) 531 [P⁺, ¹⁸⁴W]; ¹H NMR (400 MHz, C₆D₆) δ 1.92 (s, 15H, C₅Me₅), 2.62 (m, 4H, Tol Me, CH_{syn}H), 3.46 (d, ²J_{HH} = 6.6, 1H, CH_{anti}H), 5.77 (br d, 1H, Tol H), 6.59 (t, ³J_{HH} = 7.5, 1H, Bzl H_{para}), 6.79 (t, ³J_{HH} = 7.9, 1H, Tol H), 6.90 (t, ³J_{HH} = 7.9, 2H, Bzl H_{meta}), 7.07 (d, ³J_{HH} = 7.9, 1H, Tol H), 7.16 (t, ³J_{HH} = 7.9, 1H, Tol H), 7.21 (d, ³J_{HH} = 7.5, 2H, Bzl H_{ortho}); ¹³C{¹H} NMR (75 MHz, CDCl₃) δ 10.4 (C₅Me₅), 28.5 (Tol Me), 52.8 (br s, CH₂), 109.6 (C₅Me₅), 119.9 (br, Bzl C_{ipso}), 124.0, 124.8, 128.5, 129.1, 131.2, 134.3, 149.6 (Ar C), 177.7 (Tol C_{ipso}). Anal. Calcd for C₂₄H₂₉NOW: C, 54.25; H, 5.50; N, 2.64. Found: C, 54.16; H, 5.64; N, 2.74.

Cp*W(NO)(CH₂C₆H₅)(CH₂CMe₃) (12). Complex **12** was prepared via the reaction of Cp*W(NO)(CH₂CMe₃)Cl (1.0 g, 2.2 mmol) and (C₆H₅CH₂)₂Mg·x(dioxane) (0.34 g, 2.2 mmol) in Et₂O (10 mL). The crude residue was extracted with 4:1 Et₂O/hexanes (3 × 15 mL) and filtered through Celite (1 × 0.7 cm) supported on a frit. Storing the filtrate at -30 °C overnight provided **12** as yellow-orange needles (890 mg, 79%): IR (cm⁻¹) 1538 (s, ν_{NO}); MS (LREI, *m/z*, probe temperature 150 °C) 511 [P⁺, ¹⁸⁴W]; ¹H NMR (400 MHz, C₆D₆) δ -2.35 (d, ²J_{HH} = 13.4, 1H, CH_{syn}HCMCMe₃), 1.16 (s, 9H, CMe₃), 1.54 (s, 15H, C₅Me₅),

2.20 (d, ²J_{HH} = 13.4, 1H, CH_{anti}HCMCMe₃), 2.22 (d, ²J_{HH} = 8.5, 1H, CH_{syn}HPh), 2.98 (d, ²J_{HH} = 8.5, 1H, CH_{anti}HPh), 6.89 (m, 3H, Bzl H_{ortho}H_{meta}), 7.31 (t, ³J_{HH} = 7.3, 1H, Bzl H_{para}); ¹³C{¹H} NMR (50 MHz, CDCl₃) δ 10.4 (C₅Me₅), 33.8 (CMe₃), 38.4 (CMe₃), 51.7 (CH₂), 64.0 (CH₂) 109.2 (C₅Me₅), 113.3 (Bzl C_{ipso}), 127.3, 129.2, 131.8 (Bzl C_{aryl}). Anal. Calcd for C₂₂H₃₃NOW: C, 51.67; H, 6.50, N, 2.74. Found: C, 51.74; H, 6.50; N, 2.82.

Cp*W(NO)(CH₂C₆H₅)(C₆H₅) (13) and Cp*W(NO)(CHDC₆H₅)-(C₆H₅) (13-d₆). Compounds **13** and **13-d₆** were prepared via the thermolysis of **12** in benzene and benzene-*d*₆, respectively, and were isolated as red needles by crystallization from 4:1 Et₂O/hexanes.

13: 46 mg (59%); IR (cm⁻¹) 1562 (s, ν_{NO}); MS (LREI, *m/z*, probe temperature 120 °C) 517 [P⁺, ¹⁸⁴W], 487 [P⁺-NO]; ¹H NMR (400 MHz, C₆D₆) δ 1.53 (s, 15H, C₅Me₅), 2.14 (d, ²J_{HH} = 6.4, 1H, CH_{syn}H), 3.41 (d, ²J_{HH} = 6.4, 1H, CH_{anti}H), 6.50 (t, ³J_{HH} = 7.8, 2H, Bzl H_{meta}), 6.84 (d, ³J_{HH} = 7.6, 2H, Bzl H_{ortho}), 6.9–7.3 (m, Bzl H_{para}, Ph H); ¹³C{¹H} NMR (100 MHz, CDCl₃) δ 10.5 (C₅Me₅), 48.0 (CH₂), 108.9 (C₅Me₅), 113.2 (Bzl C_{ipso}), 124.1, 127.0 (Ph C_{aryl}), 129.1, 132.3, 135.7 (Bzl C_{aryl}), 138.6 (Ph C_{aryl}), 172.0 (Ph C_{ipso}). Anal. Calcd for C₂₃H₂₇NOW: C, 53.40; H, 5.26; N, 2.71. Found: C, 53.10; H, 5.36; N, 2.77.

13-d₆: (39 mg, 48%); IR (cm⁻¹) 1562 (s, ν_{NO}); MS (LREI, *m/z*, probe temperature 120 °C) 523 [P⁺, ¹⁸⁴W], 493 [P⁺-NO]; ¹H NMR (400 MHz, C₆D₆) δ 1.53 (s, 15H, C₅Me₅), 3.39 (br s, 1H, CH_{anti}D), 6.50 (t, ³J_{HH} = 7.8, 2H, Bzl H_{meta}), 6.84 (d, ³J_{HH} = 7.6, 2H, Bzl H_{ortho}), 7.31 (t, ³J_{HH} = 7.3, 1H, Bzl H_{para}); ²H{¹H} NMR (77 MHz, C₆H₆) δ 2.15 (br s, CHD_{syn}), 7.1 (m, Ph D); ¹³C{¹H} NMR (100 MHz, CDCl₃) δ 10.5 (C₅Me₅), 47.7 (t, ¹J_{CD} = 22.5 Hz, CHD), 108.9 (C₅Me₅), 113.2 (Bzl C_{ipso}), 129.1, 132.3, 135.7 (Bzl C_{aryl}), 171.8 (Ph C_{ipso}). ¹³C resonances attributable to Ph-D were not observed. Anal. Calcd for C₂₃H₂₁D₆NOW: C, 52.80; H/D, 5.20; N, 2.67. Found: C, 52.45; H/D, 4.99; N, 2.80.

Preparation of Cp*W(NO)(=CHC₆H₅)(PMe₃) (14a–b). Complexes **14a–b** were prepared by the thermolysis of **12** (75 mg, 0.15 mmol) in THF (4 mL) and PMe₃ (~20 mmol). Complex **14a** was isolated as yellow-orange blocks (38 mg, 52% yield) by crystallization from 1:2 THF/hexanes.

14a: IR (cm⁻¹) 1527 (s, ν_{NO}); MS (LREI, *m/z*, probe temperature 150 °C) 515 [P⁺, ¹⁸⁴W]; ¹H NMR (400 MHz, C₆D₆) δ 0.94 (d, ²J_{HP} = 9.0, 9H, PMe₃), 1.88 (s, 15H, C₅Me₅), 7.05 (t, ³J_{HH} = 7.3, 1H, Bzl H_{para}), 7.37 (t, ³J_{HH} = 7.6, 2H, Bzl H_{meta}), 8.06 (d, ³J_{HH} = 7.6, 2H, Bzl H_{ortho}), 12.01 (d, ³J_{HP} = 3.8, 1H, W=CH); ¹³C{¹H} NMR (75 MHz, CDCl₃) δ 11.2 (C₅Me₅), 17.8 (d, ¹J_{CP} = 34, PMe₃), 108.4 (C₅Me₅), 125.6, 128.4, 128.6 (Bzl C_{aryl}), 153.6 (d, ³J_{CP} = 3.3, Bzl C_{ipso}), 262.5 (d, ²J_{CP} = 9.6, W=CH); ³¹P NMR (81 MHz, C₆D₆) δ -8.9 (s, ¹J_{PW} = 445 Hz). NOES (400 MHz, C₆D₆) δ irradi at 0.94, NOEs at 8.06, 12.01; irradi at 1.88; NOE at 12.01. Anal. Calcd for C₂₀H₃₀NOPW: C, 46.62; H, 5.87; N, 2.72. Found: C, 46.42; H, 5.69; N, 2.95.

14b: ¹H NMR (400 MHz, C₆D₆) δ 1.08 (d, ²J_{HP} = 9.0, 9H, PMe₃), 1.80 (s, 15H, C₅Me₅), 7.05 (t, ³J_{HH} = 7.8, 1H, Bzl H_{para}), 7.10 (t, ³J_{HH} = 7.8, 2H, Bzl H_{meta}), 7.20 (d, ³J_{HH} = 7.8, 2H, Bzl H_{ortho}), 13.70 (d, ³J_{HP} = 4.4, 1H, W=CH); ¹³C{¹H} NMR (75 MHz, CDCl₃) δ 11.0 (C₅Me₅), 19.4 (d, ¹J_{CP} = 34, PMe₃), 107.8 (C₅Me₅), 124.8, 126.7, 127.9 (Bzl C_{aryl}), 153.5 (d, ³J_{CP} = 2.5, Bzl C_{ipso}), 262.5 (d, ²J_{CP} = 10.1, W=CH); ³¹P NMR (81 MHz, C₆D₆) δ -7.2 (s, ¹J_{PW} = 482 Hz). NOES (400 MHz, C₆D₆) δ irradi at 1.08, NOE at 13.70; irradi at 1.80, NOE at 7.20.

Cp*W(NO)(CH₂C₆H₅)(CH₂SiMe₃) (15). Complex **15** was prepared by the thermolysis of **12** in tetramethylsilane. The characterization data for this complex match that previously reported:³⁷ MS (LREI, *m/z*, probe temperature 150 °C) 527 [P⁺, ¹⁸⁴W]; ¹H NMR (400 MHz, C₆D₆) δ -4.06 (d, ²J_{HH} = 13.5, 1H, CH_{syn}HSiMe₃), -0.73 (d, ²J_{HH} = 13.5, 1H, CH_{anti}HSiMe₃), 0.32 (s, 9H, SiMe₃), 1.55 (s, 15H, C₅Me₅), 2.10 (d, ²J_{HH} = 5.0, 1H, CH_{syn}HPh), 3.25 (d, ²J_{HH} = 8.5, 1H, CH_{anti}H), 6.54 (d, 2H, ³J_{HH} = 7.5, 1H, Bzl H_{ortho}), 6.62 (d, 2H, ³J_{HH} = 7.5, 2H, Bzl H_{meta}), 7.50 (t, ³J_{HH} = 7.3, 1H, Bzl H_{para}); ¹³C{¹H} NMR (75 MHz, CDCl₃) δ 3.0 (SiMe₃), 10.5 (C₅Me₅), 20.0 (CH₂SiMe₃), 47.0 (CH₂Ph), 108.3 (C₅Me₅), 115.5 (Bzl C_{ipso}), 129.5, 130.4, 134.7 (Bzl C_{aryl}).

Kinetic Studies. Kinetic studies of the trapping of **1** and **1-d₄** by PMe₃ in cyclohexane were performed using a HP8452 UV-visible spectrometer equipped with a thermostated cell holder connected to a VWR1150 constant-temperature bath that is accurate to ±0.05 °C.

Table 2. X-ray Crystallographic Data for Complexes **4a**, **6**, **7a**, **8a**, and **14a**

	4a	6	7a	8a	14a
Crystal Data					
empirical formula	C ₁₈ H ₃₄ NOW	C ₁₉ H ₃₄ NOPW	C ₁₇ H ₂₇ NOW	C ₁₈ H ₂₉ NOW	C ₂₀ H ₃₀ NOPW
cryst habit, color	irregular, yellow	plate, orange	plate, yellow	irregular, yellow	block, yellow
cryst size (mm)	0.13 × 0.11 × 0.09	0.50 × 0.35 × 0.02	0.28 × 0.20 × 0.20	0.20 × 0.25 × 0.30	0.40 × 0.20 × 0.20
cryst syst	monoclinic	monoclinic	monoclinic	monoclinic	monoclinic
space group	<i>P</i> 2 ₁	<i>C</i> 2/ <i>c</i>	<i>P</i> 2 ₁ / <i>c</i>	<i>P</i> 2 ₁ / <i>n</i> (No. 14)	<i>P</i> <i>c</i> (No. 7)
vol (Å ³)	1054.83(6)	4022.4(2)	1655.88(7)	1743.5(2)	1028.93(4)
a (Å) ^a	8.5740(3)	30.6298(7)	7.5179(2)	8.4943(13)	9.5066(3)
b (Å)	13.9660(5)	8.2908(2)	13.8169(3)	13.8052(12)	8.8989(2)
c (Å)	8.9140(3)	16.6982(4)	16.1151(4)	14.9389(5)	12.5831(3)
α (deg)	90	90	90	90	90
β (deg)	98.804	108.4520(10)	98.424(1)	95.5851	104.8540(5)
γ (deg)	90	90	90	90	90
Z	2	8	4	4	2
density (calcd) (Mg/m ³)	1.559	1.675	1.786	1.751	1.663
absorptn coeff (cm ⁻¹)	55.54	58.28	69.73	66.38	57.04
<i>F</i> ₀₀₀	492	2016	872	904	508
Data Collection and Refinement					
total measd reflctns	6896	9770	8282	16138	8241
no. of unique reflctns	3562 (<i>R</i> _{int} = 0.0620)	3514 (<i>R</i> _{int} = 0.0648)	2905 (<i>R</i> _{int} = 0.0577)	4516 (<i>R</i> _{int} = 0.048)	4072 (<i>R</i> _{int} = 0.040)
final <i>R</i> indices ^b	<i>R</i> _F = 0.0404, <i>wR</i> _F = 0.0916	<i>R</i> _F = 0.0424, <i>wR</i> _F = 0.0760	<i>R</i> _F = 0.0535, <i>wR</i> _F = 0.1414	<i>R</i> _F = 0.046, <i>wR</i> _F = 0.046	<i>R</i> _F = 0.016, <i>wR</i> _F = 0.025
goodness-of-fit on <i>F</i> ^{2c}	1.059	0.963	1.012	1.87	0.89
largest diff peak and hole (e Å ⁻³)	1.270 and -1.714	1.755 and -0.932	3.601 and -2.645	2.78 and -2.69	1.29 and -1.12

^a Cell dimensions based on: **4a**, 5466 reflections, 2.31 < 2θ < 25.29°; **5**, 5497 reflections, 1.40 < 2θ < 25.06°; **6a**, 5216 reflections, 1.95 < 2θ < 25.23°. ^b Number of observed reflections: **4a**, 3092 (*I* > 2σ(*I*)); **5**, 2571 (*I* > 2σ(*I*)); **6a**, 2116 (*I* > 2σ(*I*)); **7a**, 2795 (*I* > 3σ(*I*)); **14a**, 3836 (*I* > 3σ(*I*)). *R*_F on *F* = Σ(|*F*_o - |*F*_c||)/Σ|*F*_o|; *wR*_F = [Σ(w(|*F*_o|² - |*F*_c|²)/Σ*wF*_o⁴)^{1/2}]; *w* = [σ²*F*_o² + (*AP*)² + (*BP*)²]⁻¹, where *P* = (*F*_o² + 2*F*_c²)/3 for **4a** (*A* = 0.0284, *B* = 0.0), **5** (*A* = 0.0181, *B* = 0.0) and **6a** (*A* = 0.094, *B* = 0.0); *w* = [σ²*F*_o²]⁻¹ for **7a** and **14a**. ^c GOF = [Σ(w(|*F*_o - |*F*_c||²)/(degrees of freedom)]^{1/2}.

Typical experiments were conducted using a cyclohexane solution of **1** (3 mL, 5.29 × 10⁻⁴ M) and excess PMe₃ (50 μL, 300 equiv) in a gastight quartz cuvette equipped with a Schlenk sidearm. Kinetic runs monitored the starting material band at 486 nm for no less than 3.5 half-lives. The rate constants (*k*_{obs}) were calculated using linear regression methods from plots of ln(*A*(*t*) - *A*_∞) versus time. Values of Δ*H*[‡] and Δ*S*[‡] were calculated using regression methods from plots of ln(*k*_{obs}/*T*) versus 1/*T* for the temperature range 344–371 K.

Kinetic studies of the thermolysis of **1** and **12** in benzene-*d*₆ were performed using a J. Young NMR tube charged with **1** or **12** (15 mg, 30 mmol) and 1 mL of a benzene-*d*₆ solution containing 0.5 equiv (15 mmol) of hexamethylsilane as an internal standard. The thermolysis was conducted in the constant-temperature bath, and the samples were removed at several intervals to record ¹H NMR spectra. The monitoring was performed for >3.5 half-lives, and rate constants were calculated using linear regression methods from first-order plots of the loss of starting material versus time. Studies of the isomerization of **9c** and **11c** were conducted in a similar fashion in neat benzene-*d*₆. ¹H NMR spectra were recorded at several time intervals and the percent conversions were calculated using integrations of **9a–b** product signals to the combined CMe₃ signals for **9a–c** and integrations of **11c** signals versus the combined Cp* signal for **11a–c**.

X-ray Diffraction Studies. Data collection and structure solution for complexes **4a**, **6**, and **7a** were conducted at the X-ray Crystallographic Laboratory at the University of Minnesota by Victor G. Young. Data were recorded at 173(2) K with a Siemens SMART System using graphite-monochromated Mo Kα radiation. The data were collected using the hemisphere technique to a resolution of 0.84 Å with 0.30° steps in ω. All structures were solved by direct methods, and all non-hydrogen atoms were refined anisotropically unless stated otherwise. All carbon-bound hydrogen atoms were placed in ideal positions and refined as riding atoms with individual (or group if appropriate) isotropic displacement parameters. For **4a**, racemic twinning in the crystal lattice prevented a direct solution in the space group *P*2₁. A direct-methods solution was forced in *P*2₁/*m*, which provided a contiguous molecule that was easily transformed into *P*2₁ and subsequently refined in *P*2₁. The presence of a twin caused serious problems during the final stages of refinement. The nominal structure is pseudosymmetric with its twin, thus causing the parameters of several

atom pairs in the Cp* group to be highly correlated. A total of 121 restraints were imposed to help the Cp* group become more regular (SAME, DELU, SIMU, and FLAT) and prevent C(4) (ISOR) from going nonpositive definite. The carbene, being off but close to the pseudomirror, was also restrained with DELU. For **6**, the anisotropic displacement parameters of the ring carbon atoms of the Cp* ligand were restrained to approximate rigid body motion. For **7a**, the hydride was not found and instead was placed in a physically reasonable location and refined positionally while the *U*_{iso} was tied to 1.5 times the equivalent of W(1). All calculations were performed using SGI INDY R4400-SC or Pentium computers using the SHELXTL V5.0 suite of programs.

Data collection and structure solution for complexes **8a** and **14a** were conducted at the University of British Columbia by Steven J. Rettig and Brian O. Patrick, respectively. All measurements were recorded at -93(1) °C on a Rigaku/ADSC CCD area detector using graphite-monochromated Mo Kα radiation. For **8a**, the data were collected to a maximum 2θ value of 63.6° in 0.50° oscillations with a 15.0 s exposure. A sweep of data was collected using φ oscillations from 0.0 to 190.0° at χ = -90°, and a second sweep was performed using ω oscillations between -22.0 and 18.0° at χ = -90°. The crystal-to-detector distance was 39.16 mm, and the detector swing angle was -10.00°. For **14a**, the data were collected to a maximum 2θ value of 55.8° in 0.50° oscillations with a 12.0-s exposure. A sweep of data was collected using φ oscillations from 0.0 to 190.0° at χ = 0°, and a second sweep was performed using ω oscillations between -18.0 and 23.0° at χ = 90°. The crystal-to-detector distance was 40.13(6) mm, and the detector swing angle was -5°. Both data sets were corrected for Lorentz and polarization effects. The solid-state structures were solved by heavy-atom Patterson methods and expanded using Fourier techniques. The non-hydrogen atoms were refined anisotropically. For **8a**, the metal hydride was placed in a difference map position and was not refined, and the carbon-bound hydrogen atoms were fixed in calculated positions with *d*(C–H) = 0.98 Å. For **14a**, the hydrogen atoms were included but not refined. The final cycles of full-matrix least-squares refinements were based on 4130 unique reflections and 190 variable parameters for **8a** and 3850 unique reflections and 215 variable parameters for **14a**. All calculations were performed using the teXsan crystallographic software package of Molecular Structure Corp.

X-ray crystallographic data for all five complexes are collected in Table 2, and full details of all crystallographic analyses are provided as Supporting Information.

Acknowledgment. We are grateful to the Natural Sciences and Engineering Research Council of Canada for support of this work in the form of grants to P.L. and postgraduate scholarships to C.S.A. and E.T. We also thank Drs. K. J. Ross and W. S. McNeil for stimulating and helpful discussions. Finally, we acknowledge Drs. S. J. Rettig (deceased October 27, 1998) and B. O. Patrick of this Department, and Dr. V. G.

Young of the University of Minnesota for solving the crystal structures of the representative complexes reported in this paper.

Supporting Information Available: ORTEPs and tables listing crystallographic information, atomic coordinates and *B_{eq}* values, anisotropic thermal parameters, and intramolecular bond distances, angles, and torsion angles. This material is available free of charge via the Internet at <http://pubs.acs.org>.

JA002457E